A Simultaneous Methylome and Proteome Quantitative Workflow for Complex Samples

Aaron E. Robinson,[1] Aleksandra Binek,[1] Ronald J. Holewinski,*[1] Vidya Venkatraman,[1] Sarah J. Parker,[1] Nathan Basisty,[2] Xueshu Xie,[2] Peder J. Lund,[3] Gautam Saxena,[4] José M. Mato,[5] Benjamin A. Garcia,[3] Birgit Schilling,[2] Shelly C. Lu,[6] Jennifer E. Van Eyk,[1†]*

[1]Advanced Clinical Biosystems Research Institute, The Smidt Heart Institute, Cedars Sinai Medical Center, Los Angeles, CA 90048, USA; [2]Buck Institute for Research on Aging, Novato, CA 94945, USA; [3]Department of Biochemistry and Biophysics, Epigenetics Institute, University of Pennsylvania School of Medicine, Philadelphia, PA 19104, USA; [4]DeepDIA, USA [5] CIC bioGUNE, Centro de Investigación Biomédica en Red de Enfermedades Hepáticas y Digestivas (Ciberehd), Technology Park of Bizkaia, 48160 Derio, Bizkaia, Spain; [6] Division of Digestive and Liver Diseases, Cedars-Sinai Medical Center, Los Angeles, CA, 90048, USA *Both authors contributed equally to this manuscript

† Corresponding author:

Jennifer E. Van Eyk

Jennifer.VanEyk@cshs.org

127 S. San Vicente Blvd, Advanced Health Sciences Pavilion, 9302,

The Smidt Heart Institute

Cedars-Sinai Medical Center

Los Angeles, CA 90048

Abstract

Arg and Lys undergo multiple enzymatically driven post-translational modifications (PTMs), including methylation, which is linked to key cellular processes. Today there is not a method that simultaneously accurately quantifies proteins and the methylome at the site level. We have developed a method that can differentiate an unmodified peptide from its mono-, di- or tri-methylated Arg or Lys counterpart through a data independent acquisition approach that is suitable for both triple TOF and Orbitrap mass spectrometers. This method was further expanded to include Lys acetylation and succinylation, which in conjunction with methylation allow for simultaneous quantification of Lys PTMs in a single measurement. Our approach leverages small precursor mass windows to physically separate the various methylated species within the mass spectrometer from each other during MS2 acquisition while providing accurate quantitation of low abundant peptides. To assess its biological relevance, we applied this method to a complex cellular lysate from differentially methylated in-vivo non-alcoholic steatohepatitis mouse models. We did this by first creating a biologically hyper-methylated peptide assay library, for mono-, di- and tri-methylated Lys and mono- and di-methylated Arg to which each experimental sample is compared. We further expanded the peptide assay library to include Lys acetylation and succinylation, providing the opportunity to multiplex five Lys and two Arg modification without the need for sample enrichment. In conclusion: our method, which is suitable for different mass spectrometers along with the corresponding publicly available mouse liver PTM enriched peptide assay library, provides an easily adoptable framework needed for studying global protein methylation, acetylation, and succinylation in any proteomic experiment when total protein quantification is being carried out. Wide adoption of this easy approach will allow more rapid integration of PTM studies and knowledge.

Graphical Abstract

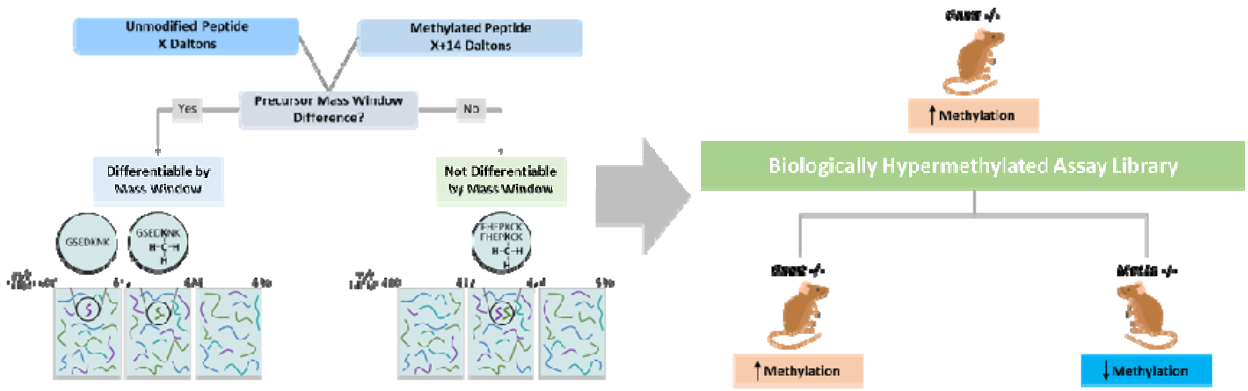

Introduction

Reversible post-translational modifications (PTMs) of proteins such as phosphorylation of Ser, Thr, and Tyr and methylation of Arg and Lys are of great interest as they act as dynamic regulators of cellular signaling.[1–3] While there have been substantial advances in biochemical methods for the detection and subsequent mass spectrometry (MS) to quantify phosphorylation (e.g., metal affinity and immunoaffinity enrichments), detection of protein methylation has lagged behind.[4,5] PhosphositePlus, a depository of PTMs identified via MS has reported 290,117 unique phosphosites while annotating only 18,394 unique methyl sites.[6] The low stoichiometry of PTM peptidoforms has been a persistent limitation to their detection in shotgun MS, particularly when data dependent precursor selection favors the more abundant peptides in a complex sample. Technological advancements in MS instrument sampling speed have expanded the dynamic range of precursor sampling for fragmentation by data dependent acquisition (DDA), and concomitantly enabled reductions in precursor window widths for data independent acquisition (DIA) based fragmentation while still maintaining reasonable cycle times. The added benefit of DIA based sampling to reduce missing data and thereby improve the consistency of peptide detection and quantitation coupled with use of PTM specific peptide assay libraries promises the continued advancement for the MS-based study of low abundant PTMs, enabling the elucidation of PTM dynamics

in complex biological systems and a more complete understanding of the complexity of cellular signaling.[4,5,7–10]

In proteins, methylation generally occurs on Arg and Lys residues with the ε-amino group of Lys being either mono, di, or trimethylated by protein Lys methyltransferases while Arg can be mono or di-methylated by protein Arg methyltransferases. In mammalian cells, S-Adenosylmethionine (SAMe) is the exclusive methyl donor for both Lys and Arg methylation.[3] Histone methylation of Lys and Arg is an integral part of the histone code known to alter the physical properties of chromatin subsequently altering gene expression.[3] Conversely, methylation of non-histone proteins has only recently emerged as a biologically relevant PTM and recent research has shown its importance in cellular signaling and function.[11–15] This information has in part been obtained from global protein methylation proteomic analysis which has recently been enabled by the development of labeling and enrichment techniques like hM SILAC, high and low pH strong cation exchange (SCX) fractionation, and utilizing peptide immunoprecipitations of methylated Lys and Arg and subsequent mass spectrometry.[16–19] However, antibody based methyl-enrichments have a number of challenges and limitations: (1) they require a large amount of sample and multiple antibodies to cover all methyl forms; (2) they often contain a sequence bias for antigen recognition, thus selectively assaying a portion of the methylome while masking an unknown but likely significant portion of methyl-sites; and (3) by nature these approaches do not enrich the unmodified form of the peptide, hindering quantification of all peptidoforms together and thus impairing the ability to study the relative abundance of PTMs.[20,21]

To overcome these limitations and facilitate a comprehensive and technically straightforward quantitative survey of the methylome in biological samples, we leveraged small precursor acquisition window DIA-MS, coupled with careful curation of a combined low pH SCX fractionated and methyl peptide immunoprecipitation enriched peptide library consisting of both unmodified and methylated peptides against which each experimental sample is extracted and compared. In addition to methylation, Lys residues can be modified by various other PTMs, including acetylation and succinylation.[22–25] To understand the extent of Lys PTMs, we expanded our DIA assay library to include succinylated and

acetylated peptides, thus providing an opportunity to quantify methylated, acetylated, succinylated, and unmodified peptides from the same sample and acquisition run. This not only allows for classical cellular protein quantification, but also provides quantification of peptidoforms containing Lys methylation, succinylation, acetylation, and Arg methylation simultaneously. This approach decreases limitations for PTM analysis as relative quantification of both total protein and three different PTMs can be obtained in the same mass spectrometry run; allowing for a technically and analytically better comparison of proteomic and relative abundance of PTM change in complex lysate across different biological conditions.

Materials and Methods

Methylated Peptide Synthesis: 100 synthesized unmodified and mono-, di- and tri-methylated peptides (JPT Peptide Technologies GmbH, Berlin, Germany) were supplied as lyophilized powder. Peptides were resuspended in 0.1% Formic Acid and pooled at 1:1 ratio, aliquoted, and stored at –80°C until used. Stabile Isotopically labeled (SIL) methyl-peptides were synthesized and were supplied as a lyophilized powder. The supplier provided product characterization (MALDI-TOF and HPLC traces) as proof of MW and purity accuracy. The peptides were of >95% purity (New England Peptide). Peptides were solubilized in 0.1% Formic Acid and pooled at 1:1 ratio, aliquoted, and stored at –80°C until used.

Liver Tissue Sample Preparation: Livers were obtained from ten-month old methionine adenosyltransferase A1 knockout (*Mat1a* -/-) male mice in a C57Bl/6 background with hepatic lipid accumulation and their aged-matched wild-type (WT) male sibling littermates,[26] and three-month old glycine *N*-methyltransferase knockout (*Gnmt* -/-) mice in a C57Bl/6 background with hepatic lipid accumulation with age matched WT littermates.[27,28] Animals were bred and housed in the CIC bioGUNE animal unit, accredited by the Association for Assessment and Accreditation of Laboratory Animal Care International. Animals were fed with standard commercial chow animal diet (Ref. 2914, Envigo, Barcelona, Spain).

Frozen mouse livers (n=6/condition) were ground to powder under liquid N2 in a cryohomoginizer (Retsch). Tissue powder was thawed and lysed in 8M urea and 100mM TRIS-HCL, pH 8.0 and samples

were ultrasonicated (QSonica) at 4 ºC for 10 min in 10 second repeating on/off intervals of 10 seconds and centrifuged at 16,000 x g for 10min at 4 ºC. The protein concentration of soluble supernatant was determined via Bicinchoninic Acid Assay (Thermo). 100µg of protein was reduced with dithiothreitol (15mM) for 1h at 37 ºC, alkylated with iodoacetamide (30mM) for 30min at room temperature in the dark, diluted to a final concentration of 2M Urea with 100mM TRIS-HCL, pH 8.0 and digested for 16 hours on a shaker at 37 ºC with a 1:40 ratio of Trypsin/Lys-C mix (Promega). Each sample was de-salted using HLB plates (Oasis HLB 30µm, 5mg sorbent, Waters).

To establish a broad methylation peptide assay library, 500ug of lysate from mouse livers (n=1/condition) was digested as described above. Each sample were de-salted (Oasis HLB, 10 mg sorbent cartridges) and SCX fractionated as described in *Kooij et al*.[29] with some modifications. De-salted peptides were dried and re-suspended in SCX buffer A (7 mM KH_2PO_4, 30% ACN, pH 2.65). The SCX columns were prepared by adding 100 mg of SCX bulk media (polysulfoethyl aspartamide, Nest Group) suspended in 1ml of 30% ACN to an empty 1 ml cartridge (Applied Separations), allowing the slurry to settle and sealing the column bed with an additional frit. The column was wet with 3 ml of 80% ACN, followed by a 3 ml H_2O wash and then equilibrated with 6 ml of SCX buffer A. Samples were loaded on the columns and the flow through was collected. Columns were washed two more times with SCX buffer A and the flowthroughs were combined as the first fraction. Samples were sequentially eluted with 1 ml SCX buffer A containing four different salt concentrations (10mM KCL, 40 mM KCl, 60mM KCL, and 150 mM KCl). All 5 fractions were dried, re-suspended in 1ml 1% FA, and desalted on using HLB plates (Oasis HLB 30µm, 5mg sorbent, Waters).

MS acquisition: MS data were acquired on either 6600 TripleTOF (Sciex) or Orbitrap Fusion Lumos (Thermo) mass spectrometers operating in DDA-MS or DIA-MS mode. iRT Standards (Biognosys) were added to each sample before acquisition.

The Orbitrap LUMOS mass spectrometer (Thermo Scientific) was equipped with an EasySpray ion source and connected to Ultimate 3000 nano LC system (Thermo Scientific). Peptides were loaded onto a PepMap RSLC C18 column (2 µm, 100 Å, 150 µm i.d. x 15 cm, Thermo) using a flow rate of 1.4 µL/min

for 7 min at 1% B (mobile phase A was 0.1% formic acid in water and mobile phase B was 0.1 % formic acid in acetonitrile) after which point they were separated with a linear gradient of 5-20%B for 45 minutes, 20-35%B for 15 min, 35-85%B for 3 min, holding at 85%B for 5 minutes and re-equilibrating at 1%B for 5 minutes. Each sample was followed by a blank injection to both clean the column and re-equilibrate at 1%B. For DIA and DDA-MS methods, the nano-source capillary temperature was set to 300 °C and the spray voltage was set to 1.8 kV. For DDA analysis MS1 scans the AGC target was set to $4x10^5$ ions with a max fill time of 50 ms. MS2 spectra were acquired using the TopSpeed method with a total cycle time of 3 seconds and an AGC target of 5x104 and a max fill time of 22 ms, and an isolation width of 1.6 Da in the quadrapole. Precursor ions were fragmented using HCD with a normalized collision energy of 30% and analyzed in the Orbitrap at 15,000K resolution. Monoisotopic precursor selection was enabled and only MS1 signals exceeding 50000 counts triggered the MS2 scans, with +1 and unassigned charge states not being selected for MS2 analysis. Dynamic exclusion was enabled with a repeat count of 1 and exclusion duration of 15 seconds.

For DIA analysis, MS1 scans were acquired in the Orbitrap at a resolution of 60,000 Hz from mass range 400-1000m/z. For MS1 scans the AGC target was set to $3x10^5$ ions with a max fill time of 50 ms. DIA MS2 scans were acquired in the Orbitrap at a resolution of 15000 Hz with fragmentation in the HCD cell at a normalized CE of 30. The MS2 AGC was set to 5e4 target ions and a max fill time of 22ms. DIA was performed using 4Da (150 scan events), 6Da (100 scan events), or 12Da (50 scan events) windows over the precursor mass range of 400-1000 m/z and the MS2 mass range was set from 100-1500 m/z. Multiplexed precursor mass window DIA acquisitions were acquired using the approach outlined in *Sidoli et al*.,[30] using 4Da and 6Da precursor mass windows outlined above.

The 6600 TripleTOF (Sciex) was connected to Eksigent 415 Liquid Chromatography (LC) system that was operated in micro-flow mode. The mobile phase A was comprised of 0.1% aqueous formic acid and mobile phase B was 0.1% formic acid in acetonitrile. Peptides were pre-loaded onto the trap column (ChromXP C18CL 10 x 0.3 mm 5 µm 120Å) at a flow rate of 10 µL/min for 3 min and separated on the analytical column (ChromXP C18CL 150 x 0.3mm 3 µm 120Å) at a flow rate of 5 µL/min using a linear

A-B gradient composed of 3-35% A for 60 min, 35-85% B for 2 min, then and isocratic hold at 85% for 5 min with re-equilibrating at 3% A for 7 min. Temperature was set to 30°C for the analytical column. Source parameters were set to the following values: Gas 1 = 15, Gas 2 = 20, Curtain Gas = 25, Source temp = 100, and Voltage = 5500V. DDA MS1 scans were acquired using a dwell time of 250 ms in the mass range of 400-1250 m/` of 100 counts per second were selected for fragmentation. DDA MS2 scans were acquired in high-sensitivity mode with dynamic accumulation with a dwell time of 25 ms for ions ranging from +2 to +5 using rolling collision energy and a collision energy spread of 5. Ions were excluded for fragmentation after one occurrence for a duration of 15 seconds.

DIA MS1 scans were acquired using a dwell time of 250 ms in the mass range of 400-1250 m/z. DIA MS2 scans were acquired over the precursor range of 400-1250 m/z with the MS2 range of 100-1800 m/z using 100 variable windows with a dwell time of 30ms. Additionally, the same samples were acquired in DIA using 4Da fixed windows over a precursor range of 400-1000 m/z with a dwell time of 22ms.

Methyl-Enrichment Sample Preparation: A cell pellet (~1 ml volume) of a hepatoma cell line derived from a *Gnmt* -/- mouse[31] was resuspended in 4 ml urea lysis buffer (8 M urea, 100 mM NaCl, 50 mM Tris pH 8) supplemented with 1X protease inhibitors (Halt, Thermo) and sonicated on ice with a probe sonicator (Fisher Sonic Dismembrator Model 100, setting 2, 3 x 15 sec). Whole cell extract was then cleared by centrifugation for 10 mins at 4°C and 14,000 rpm (15,996 x g). A total of 10 mg of protein was reduced with 10 mM dithiothreitol at 56°C for 30 mins and alkylated with 50 mM iodoacetamide for 40 mins at room temperature in the dark. After adding 4 volumes of 25 mM Tris pH 8, proteins were digested with trypsin (1/200 ratio by mass) overnight at 37°C. The digest was acidified by addition of trifluoroacetic acid (TFA) to 1% and then desalted with SepPak cartridges (3cc, 200 mg). Dried peptides were resuspended in 1 ml of phosphate-buffered saline (PBS) and dibasic sodium phosphate was added to neutralize the pH (~ 50 mM final concentration). Insoluble debris was pelleted by centrifugation for 10 mins at 17,000 x g at room temperature and the supernatant was used for immunoprecipitation of methylated peptides. Peptide concentration was estimated based on UV absorbance.

Anti-mono-methyl Lys and anti-di-methyl Lys antibodies were produced by Proteintech Group Inc. using a synthetic peptide library immunogen consisting of CX6KX6, where X is any amino acid except cysteine and the central Lys is unmodified, mono-methylated, or di-methylated. The provided anti-serum was further affinity purified in house. A total of 50 µg of each antibody per 1 mg of input peptides were combined and incubated with magnetic protein A beads (GE, 70 µl slurry per 112 µg antibody) for several hours on a rotator at 4°C. The charged beads were washed 4 x 1 ml with PBS and then incubated with 1 ml (~3.8 mg) of peptides overnight at 4°C with rotation. The beads were washed 1 x 1 ml with PBS, 1 x 1 ml with PBS supplemented with 0.8 M NaCl, 1 x 1 ml with PBS, and 1 x 1 ml with water. Captured peptides were eluted by incubation with 100 µl of 1% TFA for 5 mins at room temperature and then desalted with C18 stage tips prior to analysis by LC-MS/MS.

Methyl-Enrichment MS Acquisition: Peptides were analyzed by LC-MS/MS using a nano EasyLC 1000 system (Thermo) fitted with a fused silica column (Polymicro Tech, 75 µm i.d. x 20 cm) packed with ReproSil-Pur 120 C18-AQ (3 µm, Dr. Maisch GmbH) and positioned in line with an Orbitrap Fusion mass spectrometer (Thermo). The chromatography run consisted of a 120 min gradient increasing from 2% to 40% solvent B over 105 mins, 40% to 80% solvent B over 15 mins, and then holding at 80% solvent B for 10 mins. Water containing 0.1% formic acid and acetonitrile containing 0.1% formic acid served as solvents A and B, respectively. The mass spectrometer was programmed to perform MS1 scans in positive profile mode in the Orbitrap at 120,000 resolution covering a range of 300-1500 m/z with a maximum injection time of 100 ms and AGC target of 1e6. MS2 scans on the most intense ions, fragmented by HCD, were performed in the Orbitrap in positive centroid mode at 15,000 resolution with a maximum injection time of 200 ms, AGC target of 1e5, and NCE of 27. Quadrupole isolation was enabled with an isolation window of 2 m/z. Dynamic exclusion was set to 30 sec. MS2 scans were performed over a 3 sec cycle time.

Acetyl and Succinyl Enrichment Sample Preparation: Mitochondrial extracts and total protein lysate were prepared from mouse tissue as previously described.[25] Briefly, crude mitochondrial fractions were isolated from the livers of SIRT5-/- (C57BL/6) mice by differential centrifugation. Total protein lysate

was also isolated from the livers of WT (C57BL/6) mice. Protein concentration of mitochondrial extracts and total protein lysate was determined by BCA assay and 1 mg of protein per sample were brought to equal volumes in 8M urea in 50 mM TEAB buffer and vortexed for 10 min. Samples were reduced with 20 mM dithiothreitol for 30 min at 37C, alkylated in 40 mM iodoacetamide for 30 min at room temperature, diluted 10-fold in 50mM TEAB, and digested overnight at 37C with trypsin used at 1:50 enzyme protein. Digestion was quenched with formic acid and samples were desalted with Oasis HLB 10 mg Sorbent Cartridges, vacuum concentrated to dryness, and resuspended in 1.4mL immunoaffinity purification buffer. Immunoaffinity enrichments of modified peptides were done using the PTMScan® Acetyl-Lys Motif [Ac-K] Kit (#13416) and PTMScan® Succinyl-Lys Motif [Succ-K] Kit (#13764) (Cell Signaling Technology, Danvers, MA), using the 'One-Pot' affinity enrichment previously described.[25] For one-pot enrichments, 1 mg peptide digests were incubated in a tube containing equal parts (~62.5 µg immobilized antibody) of both the succinyl- and acetyl-Lys antibodies.

Acetyl and Succinyl Enrichment MS Acquisition: Samples were analyzed by reverse-phase HPLC-ESI-MS/MS using the Eksigent Ultra Plus nana-LC 2D HPLC system (Dublin, CA) combined with a cHiPLC System, and directly connected to a quadrupole time-of-flight SCIEX TripleTOF 5600 or a TripleTOF 6600 mass spectrometer (SCIEX, Redwood City, CA). Typically, mass resolution in precursor scans was ~35,000 (TripleTOF 5600) or 45,000 (TripleTOF 6600), while fragment ion resolution was ~15,000 in 'high sensitivity' product ion scan mode. Injected peptide mixtures initially flow into a C18 pre-column chip (200 µm x 6 mm ChromXP C18-CL chip, 3 µm, 300 Å, SCIEX) and washed at 2 µl/min for 10 min with the loading solvent (H2O/0.1% formic acid) for desalting. Subsequently, peptides flow to the 75 µm x 15 cm ChromXP C18-CL chip, 3 µm, 300 Å, (SCIEX), and eluted at a flow rate of 300 nL/min using a 3 or 4 hr gradient using aqueous and acetonitrile solvent buffers.

For the creation of a spectral library for analysis by the library-based DIA workflow, DDA acquisitions were carried out on all PTM enrichments to obtain MS/MS spectra for the 30 most abundant precursor ions (100 msec per MS/MS) following each survey MS1 scan (250 msec), yielding a total cycle time of

3.3 sec. For collision induced dissociation tandem mass spectrometry the mass window for precursor ion selection of the quadrupole mass analyzer was set to ± 1 m/z using the Analyst 1.7 (build 96) software.

Generation of Spectral Libraries and Database Searches: Assay libraries were generated as described by *Parker et al.* 2016[32] with some modifications. Briefly, DDA files were converted to mzXML and searched through the Trans Proteomic Pipeline (TPP) using 3 algorithms, (1) Comet;[33] (2) X!tandem! Native scoring;[34] and (3) X!tandem! K-scoring[35] against a reviewed, mouse canonical protein sequence database, downloaded from the Uniprot database on January 24th, 2019, containing 17,002 target proteins and 17,002 randomized decoy proteins. Peptide probability modeling was performed using the TPP peptide prophet "xinteract" and the results searches were combined using the TPP "interprophet parser". Further filtering was done using Mayu to select peptide spectral match probability values consistent with a 1% peptide false discovery rate (FDR) and a spectral library was generated using the TPP SpectraST tool. Retention times were then normalized to 'indexed' retention time space[36] using the custom python script spectrast2spectrast_irt.py, publicly available via the MSPROTEOMICSTOOLS python package (https://github.com/msproteomicstools/msproteomicstools). Biognosys internal retention time reference peptides were added to each sample immediately before acquisition and were used for retention time (RT) alignment. As needed, the expanded Common internal Retention Time standards reference peptides[37] was used to align RT in fractionated library samples, removing any outliers as described in *Parker et al. 2016*.[32,36] Retention time normalized splib files were consolidated to a single spectrum entry for each modified peptide sequence using the "consensus spectrum" function in Spectrast. These spectral libraries were then filtered to generate peptide assay libraries by selecting the top twenty most intense b or y ion fragments. The resulting file was imported into Skyline for DIA analysis as described in *Egertson et al.*[38] and was simultaneously converted to the openSWATH library input TraML format with decoys appended. The Skyline and OpenSWATH assay libraries normalized to 'indexed' retention time space and all raw files used in this study will be available at Panorama (https://panoramaweb.org/methylation_methods_1.url, Proteome Exchange ID: PXD012621) as a public resource to the proteomics community.

Quantitation of Individual Specimen by DIA-MS: Peak group extraction and FDR analysis was done as outlined in *Parker et al, 2016.*[32] Briefly, raw intensity data for peptide fragments was extracted from DIA files using the open source openSWATH workflow[39] against the sample specific peptide assay. Then, retention time prediction was made using the Biognosys iRT Standards spiked into each sample. Target and decoy peptides were then extracted. scored and analyzed using the mProphet algorithm[40] to determine scoring cut-offs consistent with 1% FDR. Peak group extraction data from each DIA file was combined using the 'feature alignment' script, which performs data alignment and modeling analysis across an experimental dataset.[41] Finally, all duplicate peptides were removed from the dataset to ensure that peptide sequences are proteotypic to a given protein in our FASTA database.

Normalization and Quantitation: The total ion current associated with the MS2 signal across the chromatogram was calculated for normalization using in-house software. This 'MS2 Signal' of each file was used to adjust the transition intensity of each peptide in a corresponding file. To obtain a measure of total protein quantity, all modified (methylated, acetylated, and succinylated) peptides were removed and analyzed separately. Normalized transition-level data of the unmodified peptides were subsequently processed using mapDIA to obtain protein level quantitation.[42] Normalized transition-level data of the all modified (methylated, acetylated, and succinylated) peptides were then analyzed individually through mapDIA to obtain peptide level quantitation of PTM containing peptides.

Data Visualization and Validation: The aligned openSWATH output was imported into Skyline[38] which was used to visualize and manually validate methylated peptides. The Skyline documents containing DIA acquisitions extracted against their respective peptide assay libraries are available at Panorama (https://panoramaweb.org/methylation_methods_1.url, Proteome Exchange ID: PXD012621).

Results

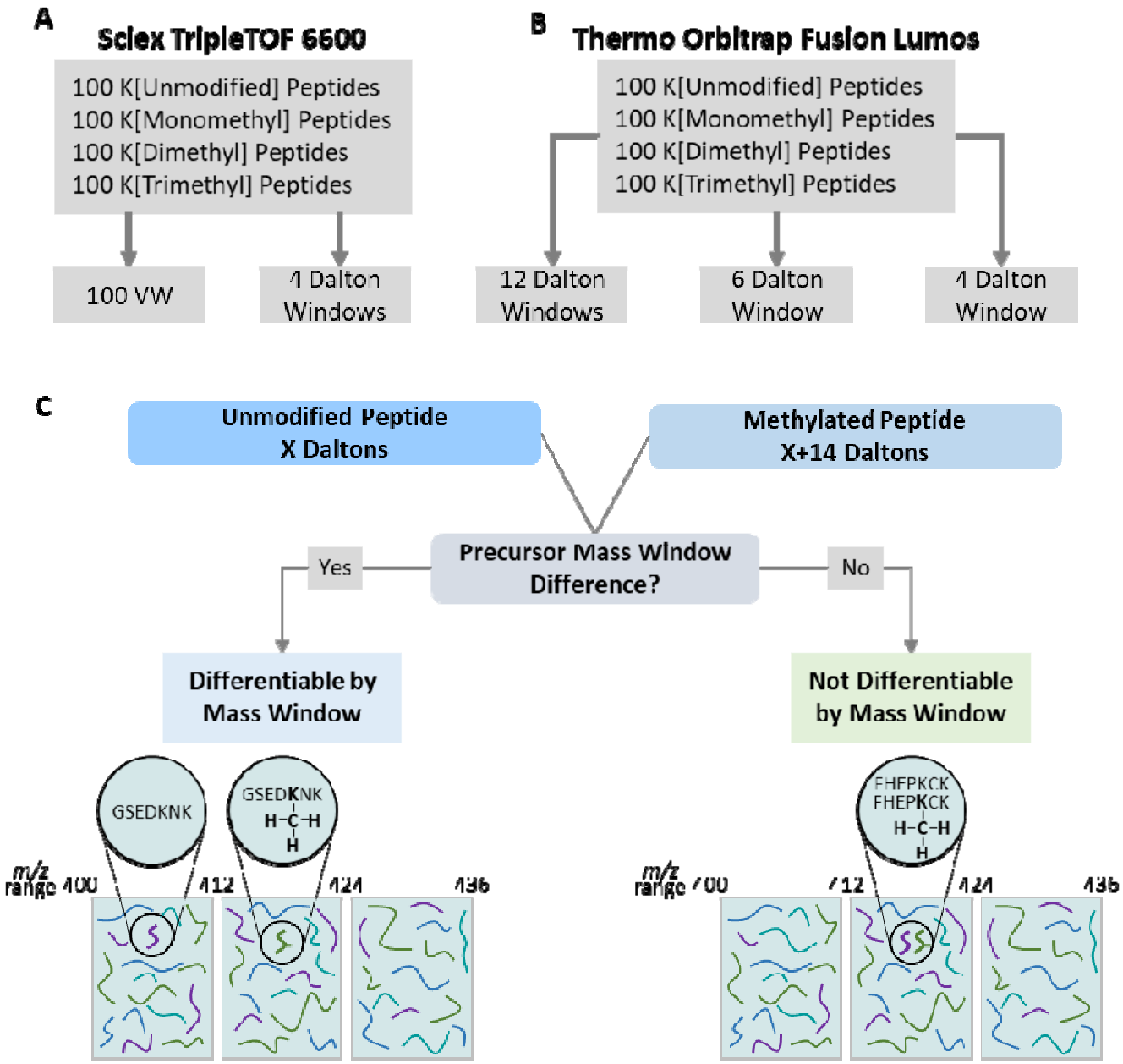

Figure 1. Schematic Overview of Experimental Design:
(A) An equimolar pool of 400 synthesized peptides containing K[Unmodified], K[Monomethyl], K[Dimethyl], and K[Trimethyl] residues were acquired in DIA on the Sciex TripleTOF 6600 with 4 Dalton and 100 Variable Window (VW) precursor mass windows. (B) Same peptide pool was acquired in DIA on the Thermo Orbitrap Fusion Lumos with 4, 6, and 12 Dalton precursor mass windows. (C) Strategy to differentiate an unmodified peptide from it's methylated form based off of precursor mass window difference. An unmodified precursor will be fragmented in a different mass window than its methylated form making it differentiable by precursor mass window.

Synthesized Methylated Peptides

The overall experimental design for quantifying protein methylation is shown in Figure 1. Although we initially focus on Lys methylation to develop the workflow, this approach is applicable to Arg methylation or any other methylated residue. To establish DIA-MS parameters to allow for differentiating a methylated peptide from an unmodified peptide, first a DDA-MS library was built on a Sciex 6600 Triple TOF based on the DDA acquisition of a pool of 400 synthesized peptides (400 femtomoles/peptide) containing either K[Unmodified], K[Monomethyl], K[Dimethyl], or K[Trimethyl]. DIA acquisitions of 400 femtomoles/peptide of the methyl peptide pool were then acquired using a 4Da precursor mass windows and 100 variable mass windows (Figure 1A). A DDA library was also created from the methyl peptide pool acquired on the Orbitrap Fusion Lumos (200 femtomoles/peptide). DIA acquisitions of 200 femtomoles/peptide were then acquired with 4, 6, and 12Da fixed precursor mass windows respectively (Figure 1B). Generally, the unmodified peptide can be physically separated from its methylated form due to precursor mass difference and thus its fragmentation in a different precursor mass window allowing for differentiation of the unmodified and methyl peptide by precursor mass window alone. However, this is not always the case and depending on precursor mass window size and the charge on the peptide the methylated peptide will fragment in the same precursor mass window as its unmodified form. In this case, a site-specific transition or a co-eluting precursor trace is necessary to correctly identify the post-translational modification (Figure 1C, Table S1). A difference in retention time cannot reliably be used to differentiate an unmodified peptide and its methyl peptidoform as 58.5% of monomethyl peptides elute within 30 seconds of each other in a 60-minute gradient while 92.7% elute within 60 seconds making separation through LC alone unpractical for DIA-MS workflows (Figure S1).

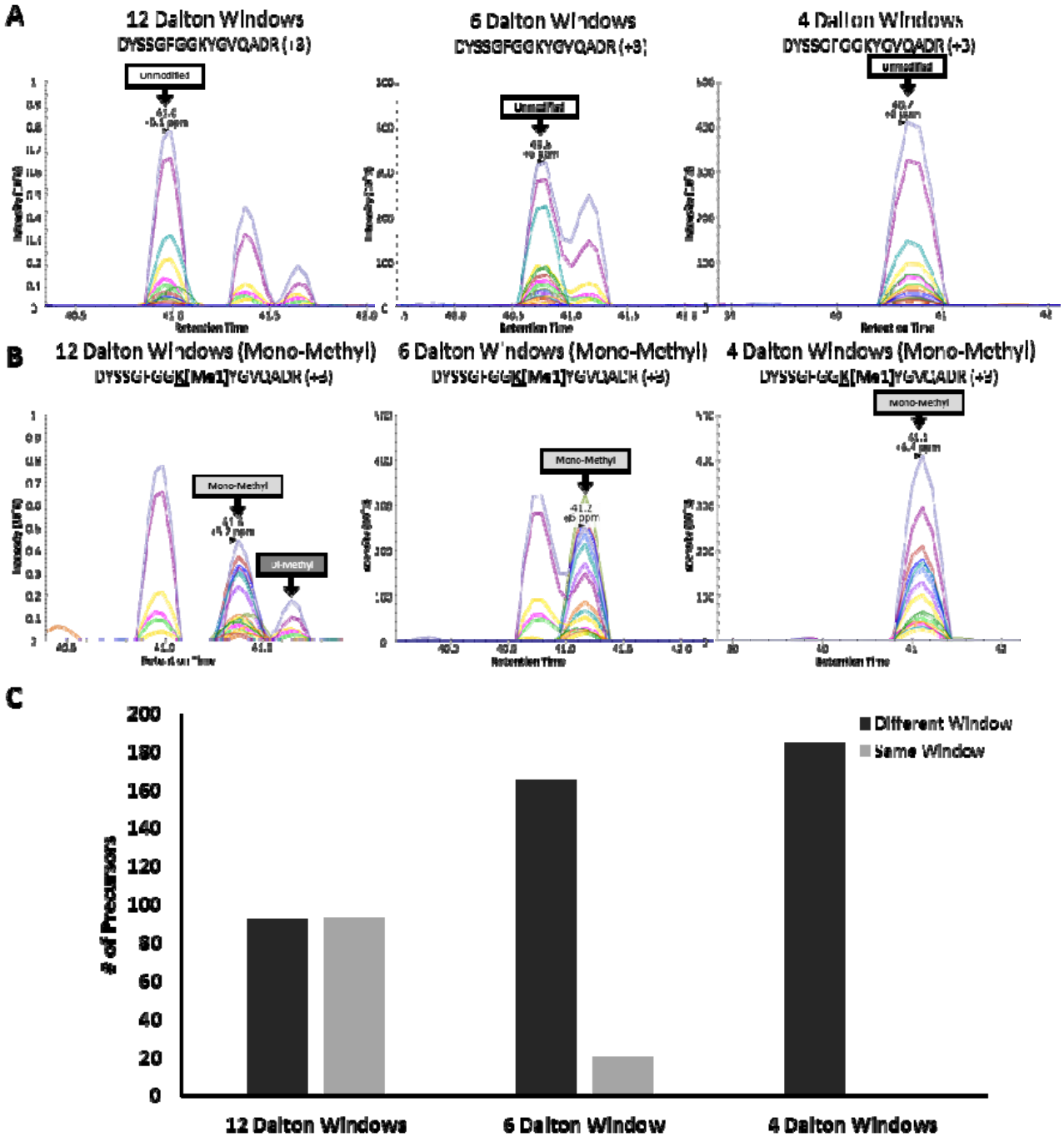

Figure 2. Synthesized Methylated Peptides: Presence of synthesized methylated and unmodified peptides acquired on the Thermo Orbitrap Fusion Lumos with 4, 6, and 12 Dalton precursor mass windows were visualized in Skyline (A) Quantified transitions of DYSSGFGGKYGVQADR (B) Quantified transitions of DYSSGFGGK[Me1]YGVQADR (C) Graphical representation of unmodified and monomethyl +2 and +3 precursors which can be differentiated from their unmodified forms using 4, 6, and 12 Dalton precursor mass windows. Black represents peptides eluting in different precursor mass windows while grey represents peptides co-eluting in the same precursor mass window.

First, we tested whether narrowing the MS1-precursor isolation window width affected the separation of different methylated peptidoforms from their unmethylated counterparts. For example, when the methyl peptide pool was acquired on the Orbitrap Lumos Fusion, we can see that with 12Da precursor mass windows three species of the same peptide have co-fragmented in the same precursor mass window. With 6Da precursor mass windows there are two species of peptide which have co-fragmented in the same window. With 4Da windows, the precursor mass window is small enough that there is only one species of the peptide found (Figure 2 A, B). With the smallest acquisition mass window schema (4Da) 100% of methylated peptides were separated from their corresponding unmodified forms. Increasing the mass window just 2 Da reduced the segregation slightly, and increasing mass window to 12Da resulted in only ~ 50% segregation of methylated peptides from unmethylated. (Figure 2C). The 4Da precursor mass windows separate 100% of both +2 and the smaller m/z +3 charged precursors from their methylated forms, whereas the commonly used 100 variable precursor mass window acquisition schema has multiple cases where 2 or more species of peptide co-fragment in the same window (Figure S2, Table S2).

In-vivo PTM DIA Assay Library

Moving next to a complex cellular lysate (liver). Two mouse models of non-alcoholic steatohepatitis (NASH) where employed, each chosen due to their extreme methylation potential. *Gnmt* -/- mice have increased SAMe and are biologically hypermethylated while *Mat1a* -/- mice are SAMe deficient and therefore hypomethylated.[26,27] First, we created a hypermethylated DIA assay library by DDA acquisitions of 5 SCX fractions from *Gnmt* -/- mouse livers. We supplemented this library with a DDA acquisition of a methyl-Lys immunoprecipitation from a hepatoma cell line derived from *Gnmt* -/- mice.[31] This gave us an assay library of 808 methyl Arg and Lys peptides. We further supplemented the library with DDA acquisitions of a 'one-pot' acetyl-Lys and succinyl-Lys immunoaffinity enrichment of mitochondrial extract and whole liver lysate isolated from WT mouse liver which provided us with 2428 succinylated peptides and 2547 acetylated peptides. We then assayed whole liver cellular lysate from *Mat1a* -/- and *Gnmt* -/- and their WT littermates against this hypermethylated Arg and Lys peptide assay library acquired in both 4Da and 12Da precursor mass windows on the Orbitrap Fusion Lumos.

Total Protein Normalization Allows for More Accurate Quantification of Methylation in NASH

After extracting 4Da precursor mass window DIA acquisition maps of *Gnmt* -/- and *Mat1a* -/- mouse liver cellular lysate against the hypermethylated DIA assay library, we quantified 78 methylated peptides with unmodified peptides quantifiable for the same protein. To determine the relative abundance of PTMs, having total protein quantification is required. Since we are using a DIA assay library containing both methylated and unmodified peptides extracted against an unenriched complex lysate, we have the ability to quantify both methylated Arg and Lys containing peptides and unmodified peptides in a single DIA acquisition. For example, a unique mono-methylated peptide corresponding to EF1A1 K165(mono-methyl) was found to be significantly increased in the hypermethylated *Gnmt* -/- NASH model compared to WT ($p<0.0005$), whereas the same site was significantly decreased in the hypomethylated *Mat1a* -/- NASH model compared to WT ($p<0.05$) (Figure 3A). After normalizing to total protein, by taking a ratio of the intensity of the methylated peptide compared to the intensity of an aggregate of all unmodified EF1A1 peptides as determined by MapDIA, *Mat1a* -/- hypomethylation compared to WT was more significant ($p<0.0005$) (Figure 3B). By being able to normalize to the aggregate protein intensity derived from unmodified peptides in the same MS acquisition we have the ability to look at Methyl/Total ratio which allows for easy normalization of the methylated peptide to the aggregate protein abundance in one DIA acquisition and can further the biological insight that one can take away from this type of data.

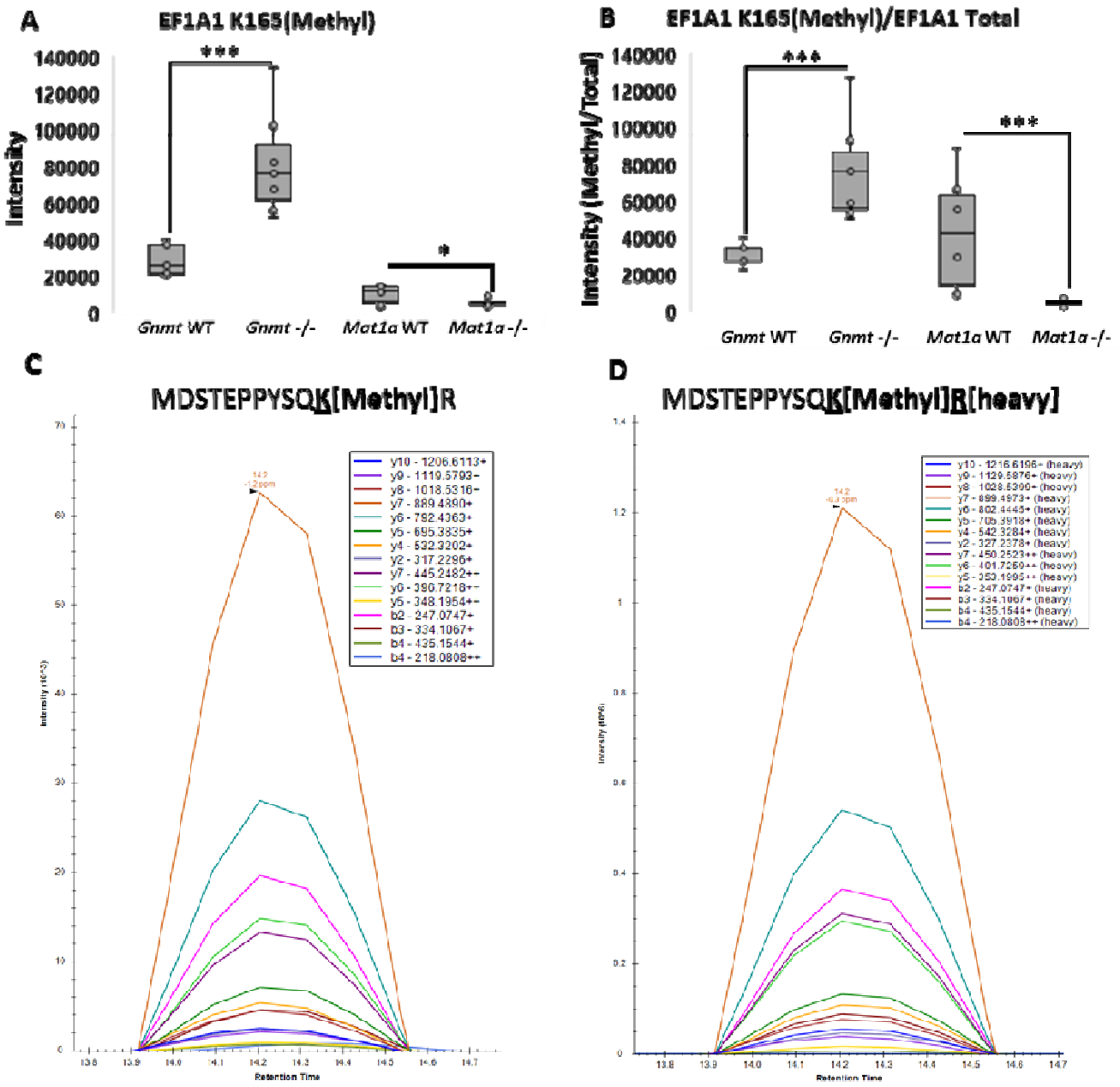

Figure 3. In-vivo Methylation: (A) Quantification of the MS2 TIC normalized intensity of peptide containing EF1A1 K[165] Mono-Methyl in *Gnmt* -/- and wild-type littermates and *Mat1a* -/- and wild-type littermates Data are box and whisker plots of six biological replicates. Two-tailed Student's t-test, $^{***}P < 0.005$, $^{*}P < 0.05$ (B) Quantification of the intensity of the MS2 TIC normalized peptide containing EF1A1 K[165] Mono-Methyl divided by the intensity of EF1A1 total protein, determined by EF1A1 unmodified peptides using MAPDIA in *Gnmt* -/- and wild-type littermates and *Mat1a* -/- and wild-type littermates Data are box and whisker plots of six biological replicates per condition. Two-tailed Student's t-test, $^{***}P < 0.0005$ (C) Skyline Visualization of the XIC of the peptide MDSTEPPYSQK[Methyl]R which corresponds to EF1A1 K[165] Mono-Methyl in *Gnmt* -/- complex liver lysate (D) Skyline Visualization of the XIC of a stably isotopically labeled peptide MDSTEPPYSQK[Methyl]R[heavy] which corresponds to EF1A1 K[165] Mono-Methyl spiked into *Gnmt* -/- complex liver lysate

To validate our methyl peptide assay library, we synthesized heavy methyl-peptides to match three proteins localized in different cellular compartments which were present in complex liver lysate from *Gnmt* -/- mice with NASH. Next, these heavy peptides were added to the *Gnmt* -/- complex liver lysate and 4Da precursor mass window DIA-MS was carried out. We found co-eluting peaks from all of the endogenous methyl-peptides and their corresponding synthetic heavy peptides (Figure 3D, Figure S3). From our SCX fractionated peptide assay library in this study, 53.7% of unmodified peptide precursors are +2 and 38.5% of precursors are +3. However, looking at only methylated precursors, only 22.2% are +2 while 58.1% of the methylated precursors are +3 (Figure S10, Table S3). This is likely due to more missed cleavages due to methylation inhibiting trypsin's ability creating longer peptides with a higher charge.[43] We can differentiate 80.3% of methylated precursors in our library from their unmodified forms due to precursor charge state of +2 and +3. When looking further into the 19.7% of peptides that remain with a charge of +4 or higher and calculating the respective precursor mass of the methylated peptide and its corresponding unmodified peptide, we can differentiate 99.1% of the remaining methylated peptides from their unmodified form by which mass window each precursor falls in leaving 0.24% (2/808) unresolvable by 4Da precursor mass windows (Table S3).

False Positive Methylation Identification in DIA-MS

Another important consideration is the extent of false positive impact on methyl-peptide identification. In other words: peptides that are in the same precursor mass window as their unmodified form, yet do not have any site-specific fragments quantified, and where the peak from the unmodified peptide is being assigned as methylated. Looking at complex cellular liver lysate from *Gnmt* -/- mice acquired with 12Da precursor mass windows, we have an example of an ambiguous identification; the same peak is being called for the methylated peptide and the unmodified peptide with no site specific transitions for the methyl-site identified (Figure 4A, B). Looking at the same sample acquired with 4Da precursor mass windows, although we can still detect the unmodified peptide, we no longer can detect the methylated peptide, proving that this is a false positive. 4Da precursor mass windows separate 100% of +2 and +3

charged precursors from their methylated forms leading to zero methylation false positive identifications in complex lysate while 12Da precursor mass windows have over 50% of ambiguous methylated peptides which are likely false positives. (Figure 4E). False positive identification also occurred for dimethyl peptides where the unmodified peak was being called as methylated based on the same criteria (Figure S4).

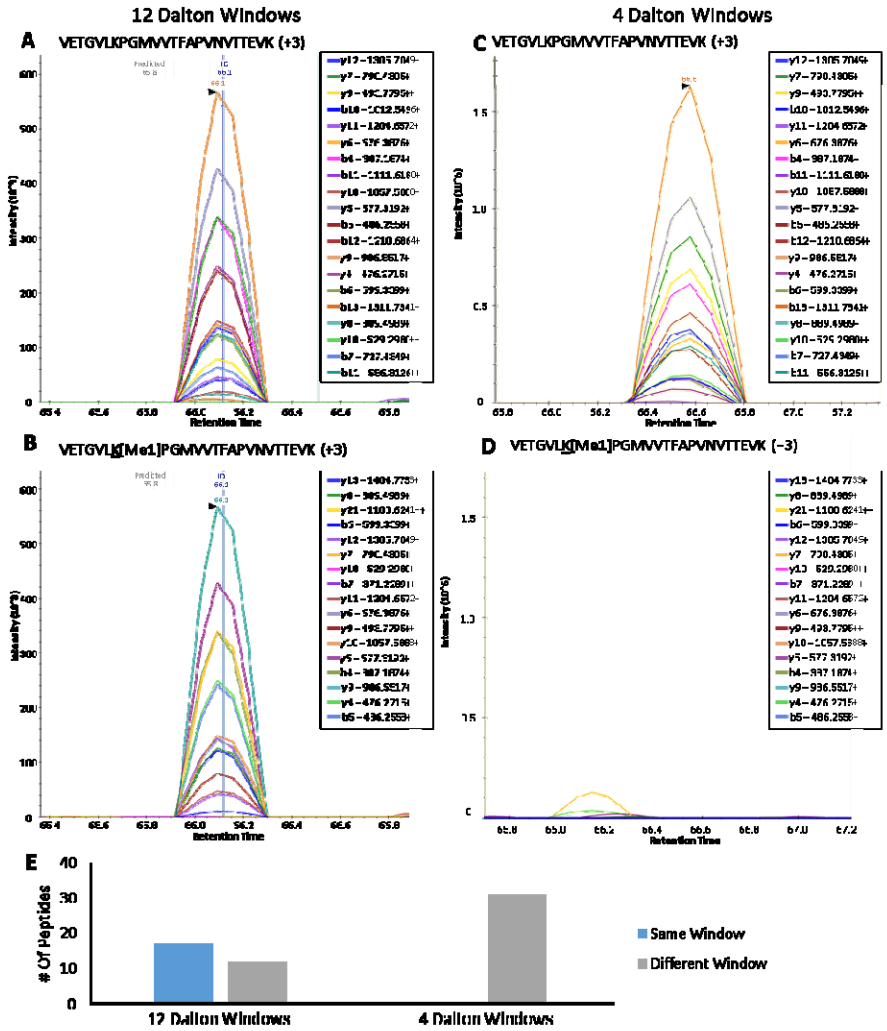

Figure 4. Methylation False Positives: Complex cellular liver lysate from *Mettl1a* -/- acquired on the Thermo Orbitrap Fusion Lumos with 4 and 12 Dalton precursor mass windows visualized in Skyline (A) Quantified transitions of VETGVLKPGMVVTFAPVNVTTEVK acquired with 12 Dalton precursor mass window (B) Quantified transitions of VETGVLK[Me1]PGMVVTFAPVNVTTEVK acquired with 12 Dalton precursor mass windows. This precursor falls in the same mass window as its unmodified form, elutes at the same time, and contains zero site specific transitions, and therefore is a false positive. (C) Quantified transitions of VETGVLKPGMVVTFAPVNVTTEVK acquired with 4 Dalton precursor mass window (D) Quantified transitions of VETGVLK[Me1]PGMVVTFAPVNVTTEVK acquired with 4 Dalton precursor mass windows. There is no discernable peak showing that the methylated peptide found with 12 Dalton precursor mass windows is a false positive.(E) Graphical representation of unmodified, monomethyl, and dimethyl +2 and +3 precursors which can be differentiated from their unmodified forms using 4 and 12 Dalton precursor mass windows. Grey represents peptides eluting in different precursor mass windows while blue represents peptides co-eluting in the same precursor mass window.

Acetylation and Succinylation are Differentially Changed in NASH Subtypes

Next, looking at acetylation and succinylation, we quantified 176 acetylated and 59 succinylated peptides in the DIA-MS runs on the mouse tissue which had unmodified peptides quantifiable of the same protein. As with methylation, to determine relative abundance of the modified peptidoform, having total protein quantification is required. By using a DIA assay library containing both modified and unmodified peptides and assaying against complex lysate, we have the ability to quantify both acetylated and succinylated Lys containing peptides and unmodified peptides in a single DIA acquisition.

A unique succinylated peptide corresponding to mitochondrial malate mehydrogenase (MDHM) K165(Succinyl) was significantly increased in the *Gnmt* -/- NASH model compared to WT ($p<0.005$) while the *Mat1a* -/- NASH model compared to WT was not significantly changed (Figure 5A). When normalizing to total protein, by taking a ratio of the intensity of the succinylated peptide compared to the intensity of unmodified MDHM peptides as determined by MapDIA, *Mat1a* -/- compared to WT became significantly decreased in the *Mat1a* -/- NASH model compared to WT ($p<0.005$) while *Gnmt* -/- NASH model compared to WT remained significant ($p<0.05$) (Figure 5B). Furthermore, a peptide proteotypic for Histone H4 (H4) with three acetyl sites, K8, K12 and K16 respectively was found in the DIA-MS datasets. This peptide was not significantly changed in either the *Gnmt* -/- NASH model compared to WT or the *Mat1a* -/- NASH model compared to WT (Figure 6A). When normalizing to total protein, by taking a ratio of the intensity of the acetylated peptide compared to the intensity of unmodified H4 peptides, *Gnmt* -/- compared to WT became significantly decreased versus WT ($p<0.05$) and *Mat1a* -/- became significantly increased compared to WT ($p<0.005$) (Figure 6B). As with methylation, being able to normalize to the protein intensity derived from unmodified peptides in the same MS acquisition we have the ability to look at Succinyl/Total or Acetyl/Total ratio which provides a more accurate representation of biological concentrations of the PTM in complex lysate.

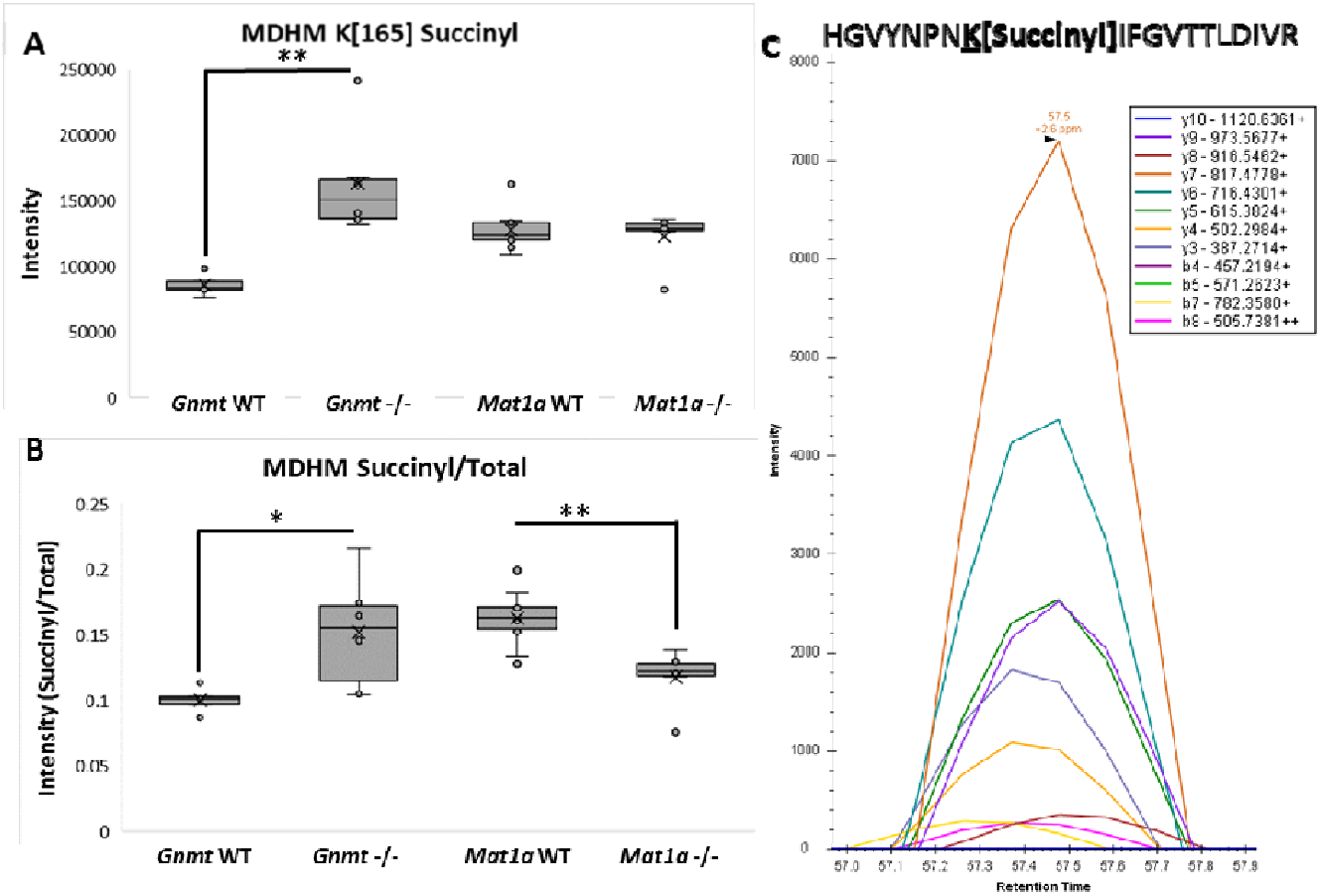

Figure 5. In-vivo Succinylation: (A) Quantification of the MS2 TIC normalized intensity of peptide containing MDHM K[165] Succinyl in *Gnmt* -/- and wild-type littermates and *Mat1a* -/- and wild-type littermates (n=6/condition) Data are box and whisker plots of six biological replicates per condition. Two-tailed Student's t-test, $^{**}P < 0.005$ (B) Quantification of the intensity of the MS2 TIC normalized peptide containing MDHM K[165] Succinyl divided by the intensity of MDHM total protein, determined by MDHM unmodified peptides using MAPDIA. Data are box and whisker plots of six biological replicates per condition. Two-tailed Student's t-test, $^{**}P < 0.005$, $^{*}P < 0.05$ (C) Skyline Visualization of the XIC of the peptide containing MDHM K[165] Succinyl

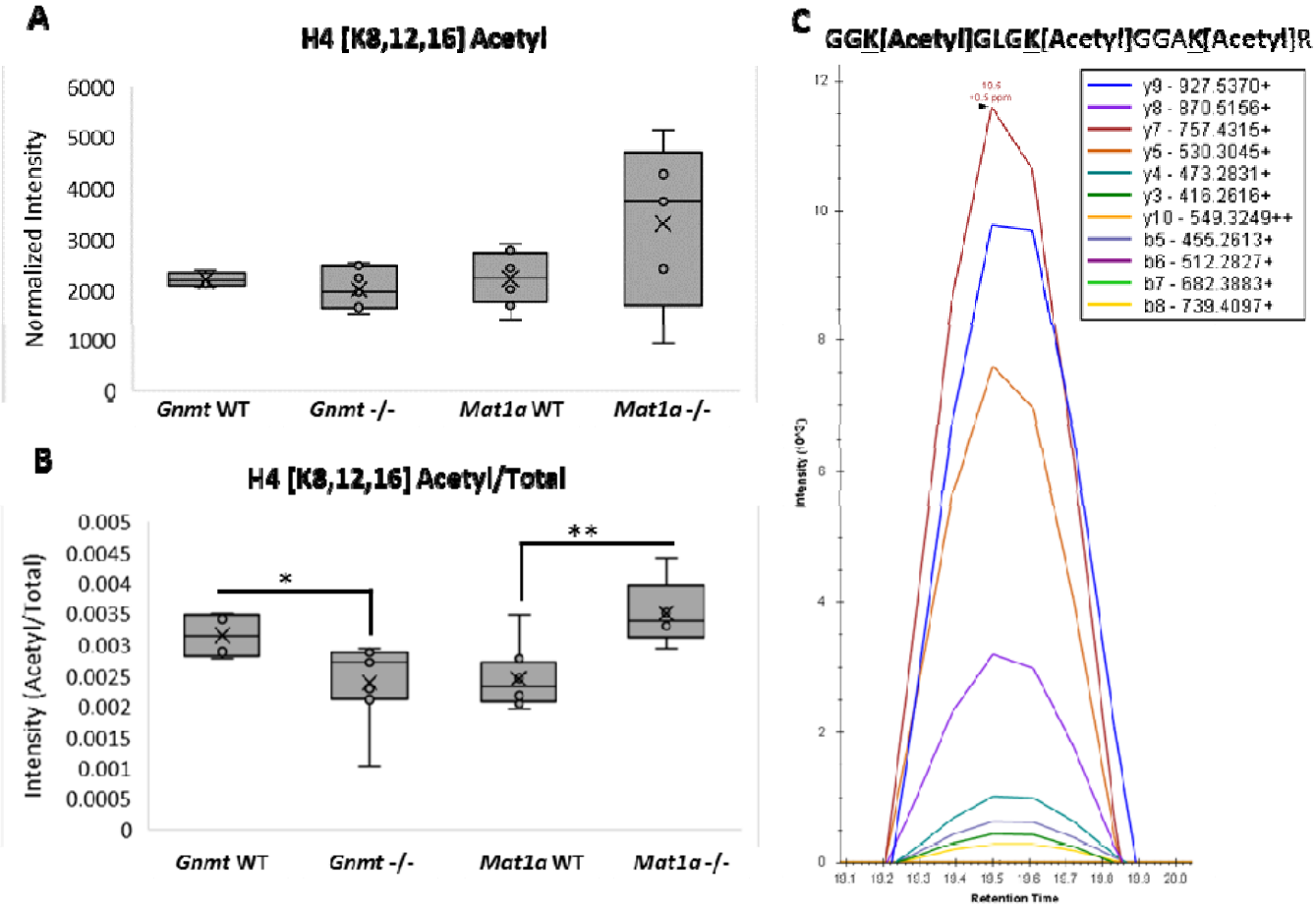

Figure 6. In vivo Acetylation: (A) Quantification of the MS2 TIC normalized intensity of a proteotypic peptide mapping to H4 K[8,12,16] Acetyl in *Gnmt* -/- and wild-type littermates and *Mat1a* -/- and wild-type littermates. Data are box and whisker plots of six biological replicates per condition. (B) Quantification of the intensity of the MS2 TIC normalized peptide containing H4 K[8,12,16] Acetyl divided by the intensity of H4 total protein, determined by H4 unmodified peptides using MAPDIA in *Gnmt* -/- and wild-type littermates and *Mat1a* -/- and wild-type littermates. Data are box and whisker plots of six biological replicates per condition. Two-tailed Student's t-test, $^{**}P < 0.005$, $^{*}P < 0.05$ (C) Skyline Visualization of the XIC of the peptide containing H4 K[8,12,16] Acetyl

We detected the presence these succinylated and acetylated peptides by showing the highest abundant transitions found in DDA and DIA acquisitions of 'one-pot' acetyl-Lys and succinyl-Lys immunoaffinity enrichment from WT mouse liver were also found in complex *Gnmt* -/- liver lysate (Figure S5, S6). Furthermore, for the tri-acetylated H4 K[9,13,17] peptide, the relative abundance of these transitions were constant between DIA acquisitions acquired on the Orbitrap Fusion Lumos and the Sciex TripleTOF

6600. Additionally, these acquisitions were run on instruments located at two different research institutes, and yet yielded the same confident identifications of an acetylated and succinylated peptide respectively.

Simultaneous Total Protein and PTM Quantification

Total protein quantification was also obtained at the same time as the PTM data because our DIA assay library was built with SCX fractionated complex cellular lysate, containing both modified peptides as well as unmodified peptides. Focusing on the total protein data from *Gnmt* -/- mice with NASH and comparing the 12Da precursor mass window data to the 4Da precursor mass window data, we achieve marginally better results when searching the 4Da precursor mass window data through OpenSWATH. Assaying against the same SCX fractionated DDA library, 5,111 proteins, 26,293 peptides, and 341,241 transitions where identified with our 4Da Precursor mass windows. With the 12Da precursor mass window acquisitions, we matched 4,595 proteins, 22,782 peptides, and 304,365 transitions. (Figure S7).

Accuracy of Peptide Quantitation in 4Da DIA Method

To establish the accuracy the peptide quantitation obtained from our 4Da precursor mass window DIA workflow, we performed a dilution series of 71 SIL peptides in complex liver lysate using both 60 and 120 minute gradients. Observation of enough MS2 spectra across the chromatographic elution profile, also termed ‘points across the peak’ is critical for estimating the area-under-the-curve (AUC) of intensity and elution time, and thus, the quantitative data for a given peptide. The more windows sampled, the more time spent in a given duty cycle, potentially sacrificing quantitative accuracy. The 4Da DIA method used in this study has a median cycle time of 6.46 seconds with 1.0% standard deviation and can detect an average of 6.94 points across a peak in a 60 minute LC gradient. Expanding the LC gradient to 120 minutes, and thus widening chromatographic peaks, an average of 10.24 points across the peak are detected (Figure S8 A,B). We next estimated the accuracy of quantification of the 4Da DIA method by examining linearity of SIL peptide AUC across the dilution series (2250fm to 7fm on column) using both 60 and 120 minute gradients. There is linearity in quantification ($r^2 > 0.95$) of 87/91 (95.6%) of transitions corresponding to precursors for the SIL peptides in the 60 gradient and linearity in quantification ($r^2 > 0.95$) for 91/91 (100%) of the transitions corresponding to precursors for the SIL peptides in the 120-

minute gradient. We additionally looked at the lower end of the dilution curve (100fm to 7fm on column) to see how the 4da DIA method performs on lower abundant peptides and found a ($r^2 > 0.95$) for 84/91 (92.3%) and 85/91 (93.4%) of the transitions corresponding to SIL precursors for the 60 minute gradient and the 120-minute gradient respectively. Furthermore, we performed a dilution series of the same 71 SIL peptides in complex liver lysate with 12Da precursor mass windows in a 120-minute gradient and found linearity in quantification ($r^2 > 0.95$) of 87/91 (95.6%) of transitions corresponding to precursors for the SIL peptides in the full dilution series. Unexpectedly, looking at the lower end of the dilution series, we found that only 59/91 (64.8%) of the transitions corresponding to SIL precursors show linearity in quantification, showing that the 4Da DIA method provides more accurate quantitation of lower abundant peptides than a 12Da DIA method on the Orbitrap Fusion Lumos (Figure S8C, Table S4).

Performance of Alternate DIA Data Analysis Methods

MS1 centric workflows like DIA-Umpire[44] and the "DirectDIA" function in Spectronaut[45] use of MS1 masses in a "spectral-centric" workflow have the ability to differentiate a modified peptide from an unmodified peptide by the precursor mass alone. However, these tools rely on a coeluting precursor trace to accurately identify a peptide. Using the SIL peptides dilution series to mimic low abundant peptides in complex liver lysate and visualizing the results in Skyline we found cases where as the concentration of SIL peptides decreased, a coeluting precursor trace was lost while transitions remained. Although 100% of SIL peptides had a coeluting precursor trace at 2250 femtomoles on column in both the 60 and 120-minute gradient, as the concentration of SIL peptides decreased so did their coeluting precursor traces; as the concentration of SIL peptides approached 7 femtomoles on column, only 36% had coeluting precursor traces in the 60 min gradient and 46% had coeluting precursor traces in 120-minute gradient (Figure S8 E,F). Accordingly, using MS1 traces of SIL peptides to determine linearity of quantitation, we found a sharp decrease in accurate quantitation at the lower end of the dilution curve in 4Da and 12Da DIA methods (Figure S8D, Table S4). Furthermore, looking at endogenous modified peptides in these same acquisitions extracted against the PTM enriched peptide assay library; methylated, acetylated, or succinylated, we found 60.4% of modified peptides do not have a coeluting precursor trace, making them

undetectable by “MS1-centric” approaches and in the case of methylated peptides undifferentiable from their unmodified peptidoform without 4Da precursor mass windows (Figure S9 A,B). To further this point, we next analyzed DIA acquisitions of complex liver lysate using a different data analysis software. We chose to use Spectronaut’s software suite as Spectronaut has the ability to analyze DIA data with a targeted library based method as well as DirectDIA, a MS1-centric library free approach. Assaying complex liver lysate DIA acquisitions against the PTM enriched DIA library resulted in quantitation of 188 endogenous modified peptides; methylated, acetylated, or succinylated. DirectDIA analysis of the same DIA acquisitions resulted in 28 endogenous modified peptides. Assaying the same complex liver lysate acquired with 12Da windows using DirectDIA resulted in 35 endogenous PTM containing peptides (Figure S9C, Table S5). Instead of relying on a coeluting precursor mass as is done with other MS analytical pipelines to identify a modified peptide and differentiate a methylated peptide from unmodified peptide, our method physically separates the unmodified and methylated peptides within the mass spectrometer by acquiring their precursors into separate mass windows. In addition, using a PTM enriched peptide assay library, our method allows for the quantitation of low abundant modified peptides without a MS1 trace.

Discussion

In this study, we have developed a DIA method utilizing 4Da precursor mass windows that is able to multiplex five Lys and two Arg modifications in complex cellular lysate without the need for sample enrichment while still allowing for total protein quantification from an aggregate of unmodified peptides. We have experimentally shown using synthesized unmodified and methylated peptides that the 4Da DIA method has the ability to physically separate 100% of the observable +2 and +3 methylated precursors from their unmodified forms. In addition, we applied the 4da DIA method to complex cellular lysate and have shown the ability of the method to quantify endogenous unmodified peptides and PTMs in a single DIA acquisition. Moreover, the 4da DIA method provides linear peptide quantitation ($r^2 > 0.95$) in both a 60 or 120 minute LC gradient and that the quantitation of the 4Da method significantly outperforms a 12Da DIA method for low abundant SIL peptides. We recommend using a 120 minute LC gradient for

future studies where quantitation is important as our method's cycle time, 6.46 seconds, achieves more points across the chromatographic peak with a longer LC gradient. Furthermore, we have shown that our publicly available PTM enriched assay library in conjunction with 4da precursor mass windows significantly outperforms MS1 centric workflows for endogenous low abundant modified and unmodified peptides. Instead of relying on a coeluting precursor trace as is done with other MS analytical pipelines to differentiate a methylated peptide from an unmodified peptide, our method physically separates the unmodified and methylated peptides by acquiring each precursor in a separate mass window allowing for the quantitation of low abundant modified peptides without the presence of a precursor trace.

We have further shown that our method can be expanded to quantify Lys methylation, acetylation, and succinylation in a single DIA acquisition. The ability to assay multiple biologically relevant Lys PTMs not only provides an opportunity to quantify methylated, acetylated, and succinylated peptides from the same sample and acquisition run but also gives insight into the importance of Lys PTM crosstalk. Lys residues can be modified by multiple PTMs and crosstalk between these PTMs constitutes a major regulatory mechanism of protein function.[22–24] Despite its importance in biology, PTM crosstalk is difficult to study and currently not possible with without enrichment of each respective PTM. Using our approach, we can assay 946 Lys residues which contain multiple PTMs; 24 Lys residues contain multiple methyl forms (Figure S121) and 922 Lys residues where crosstalk between acetylation, succinylation, or methylation occurs, 872 of which have crosstalk between acetylation and succinylation (Figure S11B). Having the ability to simultaneously identify and quantify peptides with Lys PTM crosstalk will further our understanding of the role of PTM crosstalk in biological systems.

A previous study by *Sidoli et. al.*, also has applied small precursor mass windows to analyze methylation from histone enriched lysate using multiplexed 6Da precursor mass windows which have the ability to differentiate a +2 precursor from its unmodified form but not a +3 precursor.[30] We compared multiplexed 4 and 6Da precursor mass windows using the approach outlined in *Sidoli et al*., to non-multiplexed windows on our *Gnmt* -/- complex liver lysate. Although we were able to find methylated peptides, the intensity was on average 10 fold lower than our 4Da precursor mass window method. The fragment ions

do not perfectly overlap causing issues with identification and quantitation of the peaks (Figure S12). Combined with the long time needed for data analysis to de-multiplex windows with current tools, we chose to not use that method for this study.

There are some limitations with our approach. As with most shotgun analyses of complex samples, the proteome depth is limited unless fractionation or some form of enrichment is used, and we are only able to detect the highest abundant methylated, succinylated, and acetylated peptides in complex lysate. However, we feel that the ability to quantitate highly abundant modified peptides as well as total protein quantitation from the same DIA acquisition provides a complementary and analytically valuable alternative despite the limited depth. Another caveat with our strategy is that although the unmodified peptide is always in a different mass window as the methylated peptide, if the unmethylated counterpart sequence contains a methionine, there is a chance that the oxidized methionine species will end up in the same precursor mass window as the methylated peptide. In this situation, quantification of a site-specific transition or a co-eluting precursor trace is needed to verify correct precursor mass. In this case, a retention time difference is a valuable method for further peptidoform differentiation, as peptides containing an oxidized methionine elute before their corresponding unmodified peptide by 2.37% ACN 'gradient units'.[46] By looking at either the retention time difference from the unmodified peptide, a co-eluting precursor trace, or by having a site specific transition, one can easily differentiate a methylated peptide from an oxidized peptide. Additional consideration should be taken when comparing tri-methylated and acetylated peptides. Acetylation of ε-amino groups of Lys results in shifted retention time with respect to their unmodified counterpart sequences whereas tri-methylation does not.[47] Furthermore, high mass accuracy instrumentation can distinguish these isobaric modifications.[48] Therefore the combination of relative retention time shifts with site-specific transitions allows for the unequivocal determination of trimethylation vs. acetylation. Finally, a methylated Lys or Arg often inhibits trypsin's ability to cleave. In order to determine the stochiometric site specific ratio of a modified peptidoform, we ideally would use an enzyme that would give a methylated peptide without any missed cleavages and normalize to the intensity of the unmodified peptide which would give a better representation of the

quantity of the modified peptidoform than our approach. However, to make our method for methylation quantitation more useful for the proteomics community as a whole, we decided to use Trypsin for our study as it is currently the most commonly used endoproteinase in the field.

The small precursor mass window DIA approach outlined in this study which is suitable for both triple TOF and Orbitrap mass spectrometers along with the corresponding publicly available hypermethylated, acetylated, and succinylated mouse liver methyl peptide assay library provides an easily adoptable framework needed for studying global protein methylation, acetylation, and succinylation as well as total protein quantification in any DIA proteomic experiment without the need for enrichment of each experimental sample. This approach opens up the possibility for studying PTM's from small experimental samples like tissue biopsies where there isn't enough sample for traditional methyl-immunoprecipitations. Wide adoption of this easy approach will allow more rapid integration of methylation studies in DIA proteomic experiments and increase the knowledge of the role of methylation in complex biological systems.

Conclusion:

In this study we have developed a DIA method utilizing 4Da precursor mass windows that is able to differentiate all forms of methylated peptides from their unmodified forms using synthesized methylated peptides. We then interrogated this novel method on in-vivo complex cellular lysate using a hypermethylated mouse liver assay library which can be used as a community resource. We have shown that we are able to detect and quantify protein methylation from our approach in two differentially methylated in-vivo mouse models of NASH as well as quantify Lys acetylation, succinylation, and total protein from the same sample. At the same time, we can obtain both site specific methylation, acetylation, succinylation, and total protein quantity allowing for the determination of relative ratio for each modified peptidoform. Overall, our study describes a novel approach to simultaneously quantify protein methylation, acetylation, succinylation, and total protein in in-vivo complex cellular lysate in one DIA acquisition without the need for enrichment of each biological sample.

Author Contributions

The manuscript was written through contributions of all authors. All authors have given approval to the final version of the manuscript.

ACKNOWLEDGMENT

The authors thank Helen Choi for helping with figure design. This work was supported by USA National Institutes of Health (NIH) grants R01DK107288 (SC Lu and J Van Eyk), NIH GM110174 and AI118891 (B Garcia), and Agencia Estatal de Investigación MINECO SAF 2017-88041-R, ISCiii PIE14/00031 CIBERehd-ISCiii, and Severo Ochoa Excellence Accreditation SEV-2016-0644) (J Mato).

ABBREVIATIONS

PTMs	Post translational modifications
MS	Mass spectrometry
DDA	Data Dependent Acquisition
DIA	Data independent acquisitions
SAMe	S-Adenosylmethionine
SILAC	Stable Isotope Labeling with Amino Acids in Cell Culture
SCX	Strong Cation Exchange
SIL	Stabile Isotopically Labeled
Mat1a -/-	Methionine Adenosyltransferase A1 knockout
WT	Wild-type
Gnmt -/-	Glycine *N*-methyltransferase knockout
PBS	Phosphate-buffered saline
LC	Liquid Chromatography
TPP	Trans Proteomic Pipeline
FDR	False discovery rate
NASH	Non-alcoholic steatohepatitis
AUC	area-under-the-curve

FIGURE LEGENDS

Figure 1. Schematic Overview of Experimental Design: (A) An equimolar pool of 400 synthesized peptides containing K[Unmodified], K[Monomethyl], K[Dimethyl], and K[Trimethyl] residues were acquired in DIA on the Sciex TripleTOF 6600 with 4Da and 100 Variable Window (VW) precursor mass windows. (B) Same peptide pool was acquired in DIA on the Thermo Orbitrap Fusion Lumos with 4, 6, and 12Da precursor mass windows. (C) Strategy to differentiate an unmodified peptide from its methylated form based off of precursor mass window difference. An unmodified precursor will be

fragmented in a different mass window than its methylated form making it differentiable by precursor mass window.

Figure 2. Synthesized Methylated Peptides: Presence of synthesized methylated and unmodified peptides acquired on the Thermo Orbitrap Fusion Lumos with 4, 6, and 12Da precursor mass windows were visualized in Skyline (A) Quantified transitions of DYSSGFGGKYGVQADR (B) Quantified transitions of DYSSGFGGK[Me1]YGVQADR (C) Graphical representation of unmodified and monomethyl +2 and +3 precursors which can be differentiated from their unmodified forms using 4, 6, and 12Da precursor mass windows. Black represents peptides eluting in different precursor mass windows while grey represents peptides co-eluting in the same precursor mass window.

Figure 3. In-vivo Methylation: (A) Quantification of the MS2 TIC normalized intensity of peptide containing Elongation factor 1-alpha 1 (EF1A1) K[165] Mono-Methyl in Gnmt -/- and wild-type littermates and Mat1a -/- and wild-type littermates Data are box and whisker plots of six biological replicates. Two-tailed Student's t-test, $***P < 0.005$, $*P < 0.05$ (B) Quantification of the intensity of the MS2 TIC normalized peptide containing EF1A1 K[165] Mono-Methyl divided by the intensity of EF1A1 total protein, determined by EF1A1 unmodified peptides using MAPDIA in Gnmt -/- and wild-type littermates and Mat1a -/- and wild-type littermates Data are box and whisker plots of six biological replicates per condition. Two-tailed Student's t-test, $***P < 0.0005$ (C) Skyline Visualization of the XIC of the peptide MDSTEPPYSQK[Methyl]R which corresponds to EF1A1 K[165] Mono-Methyl in Gnmt -/- complex liver lysate (D) Skyline Visualization of the XIC of a stably isotopically labeled peptide MDSTEPPYSQK[Methyl]R[heavy] which corresponds to EF1A1 K[165] Mono-Methyl spiked into Gnmt -/- complex liver lysate

Figure 4. Methylation False Positives: Complex cellular liver lysate from *Mat1a* -/- acquired on the Thermo Orbitrap Fusion Lumos with 4Da and 12Da precursor mass windows visualized in Skyline (A) Quantified transitions of VETGVLKPGMVVTFAPVNVTTEVK acquired with 12Da precursor mass window (B) Quantified transitions of VETGVL**K[Methyl]**PGMVVTFAPVNVTTEVK acquired with

12Da precursor mass windows. This precursor falls in the same mass window as its unmodified form, elutes at the same time, and contains zero site specific transitions, and therefore is a false positive. (C) Quantified transitions of VETGVLKPGMVVTFAPVNVTTEVK acquired with 4Da precursor mass window (D) Quantified transitions of VETGVL**K[Methyl]**PGMVVTFAPVNVTTEVK acquired with 4Da precursor mass windows. There is no discernable peak showing that the methylated peptide found with 12Da precursor mass windows is a false positive.(E) Graphical representation of unmodified, monomethyl, and dimethyl +2 and +3 precursors which can be differentiated from their unmodified forms using 4 and 12Da precursor mass windows. Grey represents peptides eluting in different precursor mass windows while blue represents peptides co-eluting in the same precursor mass window.

Figure 5. In-vivo Succinylation: (A) Quantification of the MS2 TIC normalized intensity of peptide containing MDHM K[165] Succinyl in *Gnmt* -/- and wild-type littermates and *Mat1a* -/- and wild-type littermates (n=6/condition) Data are box and whisker plots of six biological replicates per condition. Two-tailed Student's t-test, $^{**}P < 0.005$ (B) Quantification of the intensity of the MS2 TIC normalized peptide containing MDHM K[165] Succinyl divided by the intensity of MDHM total protein, determined by MDHM unmodified peptides using MAPDIA. Data are box and whisker plots of six biological replicates per condition. Two-tailed Student's t-test, $^{**}P < 0.005$, $^{*}P < 0.05$ (C) Skyline Visualization of the XIC of the peptide containing MDHM K[165] Succinyl

Figure 6. In-vivo Acetylation: (A) Quantification of the MS2 TIC normalized intensity of a proteotypic peptide mapping to H4 K[8,12,16] Acetyl in *Gnmt* -/- and wild-type littermates and *Mat1a* -/- and wild-type littermates. Data are box and whisker plots of six biological replicates per condition. (B) Quantification of the intensity of the MS2 TIC normalized peptide containing H4 K[8,12,16] Acetyl divided by the intensity of H4 total protein, determined by H4 unmodified peptides using MAPDIA in *Gnmt* -/- and wild-type littermates and *Mat1a* -/- and wild-type littermates. Data are box and whisker plots of six biological replicates per condition. Two-tailed Student's t-test, $^{**}P < 0.005$, $^{*}P < 0.05$ (C) Skyline Visualization of the XIC of the peptide containing H4 K[8,12,16] Acetyl

REFERENCES

1. Deribe, Y. L., Pawson, T. & Dikic, I. Post-translational modifications in signal integration. *Nat. Struct. Mol. Biol.* **17**, 666–672 (2010).

2. Murn, J. & Shi, Y. The winding path of protein methylation research: milestones and new frontiers. *Nat. Rev. Mol. Cell Biol.* **18**, 517–527 (2017).

3. Biggar, K. K. & Li, S. S.-C. Non-histone protein methylation as a regulator of cellular signalling and function. *Nat. Rev. Mol. Cell Biol.* **16**, 5 (2014).

4. Ballif, B. A., Carey, G. R., Sunyaev, S. R. & Gygi, S. P. Large-scale identification and evolution indexing of tyrosine phosphorylation sites from murine brain. *J. Proteome Res.* **7**, 311–318 (2008).

5. Montoya, A., Beltran, L., Casado, P., Rodríguez-Prados, J.-C. & Cutillas, P. R. Characterization of a TiO2 enrichment method for label-free quantitative phosphoproteomics. *Methods San Diego Calif* **54**, 370–378 (2011).

6. Hornbeck, P. V. *et al*. PhosphoSitePlus, 2014: mutations, PTMs and recalibrations. *Nucleic Acids Res.* **43**, D512–D520 (2015).

7. Mann, M. & Jensen, O. N. Proteomic analysis of post-translational modifications. *Nat. Biotechnol.* **21**, 255–261 (2003).

8. Aebersold, R. & Mann, M. Mass-spectrometric exploration of proteome structure and function. *Nature* **537**, 347–355 (2016).

9. Rosenberger, G. *et al.* Inference and quantification of peptidoforms in large sample cohorts by SWATH-MS. *Nat. Biotechnol.* **35**, 781–788 (2017).

10. Collins, B. C. *et al.* Quantifying protein interaction dynamics by SWATH mass spectrometry: application to the 14-3-3 system. *Nat. Methods* **10**, 1246–1253 (2013).

11. Paik, W. K., Paik, D. C. & Kim, S. Historical review: the field of protein methylation. *Trends Biochem. Sci.* **32**, 146–152 (2007).

12. Boisvert, F.-M., Rhie, A., Richard, S. & Doherty, A. J. The GAR motif of 53BP1 is arginine methylated by PRMT1 and is necessary for 53BP1 DNA binding activity. *Cell Cycle Georget. Tex* **4**, 1834–1841 (2005).

13. Dhayalan, A., Kudithipudi, S., Rathert, P. & Jeltsch, A. Specificity analysis-based identification of new methylation targets of the SET7/9 protein lysine methyltransferase. *Chem. Biol.* **18**, 111–120 (2011).

14. Swiercz, R., Cheng, D., Kim, D. & Bedford, M. T. Ribosomal protein rpS2 is hypomethylated in PRMT3-deficient mice. *J. Biol. Chem.* **282**, 16917–16923 (2007).

15. Wang, K. *et al.* Antibody-Free Approach for the Global Analysis of Protein Methylation. *Anal. Chem.* **88**, 11319–11327 (2016).

16. Cao, X.-J., Arnaudo, A. M. & Garcia, B. A. Large-scale global identification of protein lysine methylation in vivo. *Epigenetics* **8**, 477–485 (2013).

17. Uhlmann, T. *et al.* A Method for Large-scale Identification of Protein Arginine Methylation. *Mol. Cell. Proteomics* **11**, 1489–1499 (2012).

18. Wang, Q., Liu, Z., Wang, K., Wang, Y. & Ye, M. A new chromatographic approach to analyze methylproteome with enhanced lysine methylation identification performance. *Anal. Chim. Acta* **1068**, 111–119 (2019).

19. Larsen, S. C. *et al.* Proteome-wide analysis of arginine monomethylation reveals widespread occurrence in human cells. *Sci. Signal.* **9**, rs9 (2016).

20. Gayatri, S. *et al.* Using oriented peptide array libraries to evaluate methylarginine-specific antibodies and arginine methyltransferase substrate motifs. *Sci. Rep.* **6**, (2016).

21. Cornett, E. M. *et al.* A functional proteomics platform to reveal the sequence determinants of lysine methyltransferase substrate selectivity. *Sci. Adv.* **4**, eaav2623 (2018).

22. Horita, H., Law, A. & Middleton, K. Utilizing Optimized Tools to Investigate PTM Crosstalk: Identifying Potential PTM Crosstalk of Acetylated Mitochondrial Proteins. *Proteomes* **6**, (2018).

23. Yang, X.-J. & Seto, E. Lysine Acetylation: Codified Crosstalk with Other Posttranslational Modifications. *Mol. Cell* **31**, 449–461 (2008).

24. Xu, H.-D., Wang, L.-N., Wen, P.-P., Shi, S.-P. & Qiu, J.-D. Site-Specific Systematic Analysis of Lysine Modification Crosstalk. *Proteomics* **18**, e1700292 (2018).

25. Basisty, N., Meyer, J. G., Wei, L., Gibson, B. W. & Schilling, B. Simultaneous Quantification of the Acetylome and Succinylome by 'One□Pot' Affinity Enrichment. *Proteomics* **18**, (2018).

26. Alonso, C. *et al.* Metabolomic Identification of Subtypes of Nonalcoholic Steatohepatitis. *Gastroenterology* **152**, 1449-1461.e7 (2017).

27. Varela-Rey, M. *et al.* Fatty liver and fibrosis in glycine N-methyltransferase knockout mice is prevented by nicotinamide. *Hepatol. Baltim. Md* **52**, 105–114 (2010).

28. Luka, Z., Capdevila, A., Mato, J. M. & Wagner, C. A glycine N-methyltransferase knockout mouse model for humans with deficiency of this enzyme. *Transgenic Res.* **15**, 393–397 (2006).

29. Kooij, V., Holewinski, R. J., Murphy, A. M. & Van Eyk, J. E. Characterization of the Cardiac Myosin Binding Protein-C Phosphoproteome in Healthy and Failing Human Hearts. *J. Mol. Cell. Cardiol.* **60**, 116–120 (2013).

30. Sidoli, S., Fujiwara, R. & Garcia, B. A. Multiplexed data independent acquisition (MSX-DIA) applied by high resolution mass spectrometry improves quantification quality for the analysis of histone peptides. *Proteomics* **16**, 2095–2105 (2016).

31. Martínez-López, N. *et al.* Hepatoma Cells from Mice Deficient in Glycine N-Methyltransferase Have Increased RAS Signaling and Activation of Liver Kinase B1. *Gastroenterology* **143**, 787-798.e13 (2012).

32. Parker, S. J., Venkatraman, V. & Van Eyk, J. E. Effect of peptide assay library size and composition in targeted data-independent acquisition-MS analyses. *Proteomics* **16**, 2221–2237 (2016).

33. Eng, J. K., Jahan, T. A. & Hoopmann, M. R. Comet: an open-source MS/MS sequence database search tool. *Proteomics* **13**, 22–24 (2013).

34. Craig, R. & Beavis, R. C. TANDEM: matching proteins with tandem mass spectra. *Bioinforma. Oxf. Engl.* **20**, 1466–1467 (2004).

35. MacLean, B., Eng, J. K., Beavis, R. C. & McIntosh, M. General framework for developing and evaluating database scoring algorithms using the TANDEM search engine. *Bioinforma. Oxf. Engl.* **22**, 2830–2832 (2006).

36. Escher, C. *et al.* Using iRT, a normalized retention time for more targeted measurement of peptides. *Proteomics* **12**, 1111–1121 (2012).

37. Parker, S. J. *et al.* Identification of a Set of Conserved Eukaryotic Internal Retention Time Standards for Data-independent Acquisition Mass Spectrometry. *Mol. Cell. Proteomics MCP* **14**, 2800–2813 (2015).

38. Egertson, J. D., MacLean, B., Johnson, R., Xuan, Y. & MacCoss, M. J. Multiplexed Peptide Analysis using Data Independent Acquisition and Skyline. *Nat. Protoc.* **10**, 887–903 (2015).

39. Röst, H. L. *et al.* OpenSWATH enables automated, targeted analysis of data-independent acquisition MS data. *Nat. Biotechnol.* **32**, 219–223 (2014).

40. Reiter, L. *et al.* mProphet: automated data processing and statistical validation for large-scale SRM experiments. *Nat. Methods* **8**, 430–435 (2011).

41. Röst, H. L. *et al.* TRIC: an automated alignment strategy for reproducible protein quantification in targeted proteomics. *Nat. Methods* **13**, 777–783 (2016).

42. Teo, G. *et al.* mapDIA: Preprocessing and statistical analysis of quantitative proteomics data from data independent acquisition mass spectrometry. *J. Proteomics* **129**, 108–120 (2015).

43. Ong, S.-E., Mittler, G. & Mann, M. Identifying and quantifying *in vivo* methylation sites by heavy methyl SILAC. *Nat. Methods* **1**, 119–126 (2004).

44. DIA-Umpire: comprehensive computational framework for data-independent acquisition proteomics | Nature Methods. Available at: https://www.nature.com/articles/nmeth.3255. (Accessed: 16th July 2019)

45. Bruderer, R. *et al*. Extending the Limits of Quantitative Proteome Profiling with Data-Independent Acquisition and Application to Acetaminophen-Treated Three-Dimensional Liver Microtissues. *Mol. Cell. Proteomics MCP* **14**, 1400–1410 (2015).

46. Lao, Y. W. *et al.* Chromatographic behavior of peptides containing oxidized methionine residues in proteomic LC–MS experiments: Complex tale of a simple modification. *J. Proteomics* **125**, 131–139 (2015).

47. Yang, L. *et al.* Unambiguous Determination of Isobaric Histone Modifications by Reversed-Phase Retention Time and High-Mass Accuracy. *Anal. Biochem.* **396**, 13–22 (2010).

48. Zhang, L., Eugeni, E. E., Parthun, M. R. & Freitas, M. A. Identification of novel histone post-translational modifications by peptide mass fingerprinting. *Chromosoma* **112**, 77–86 (2003).

Graphical Abstract

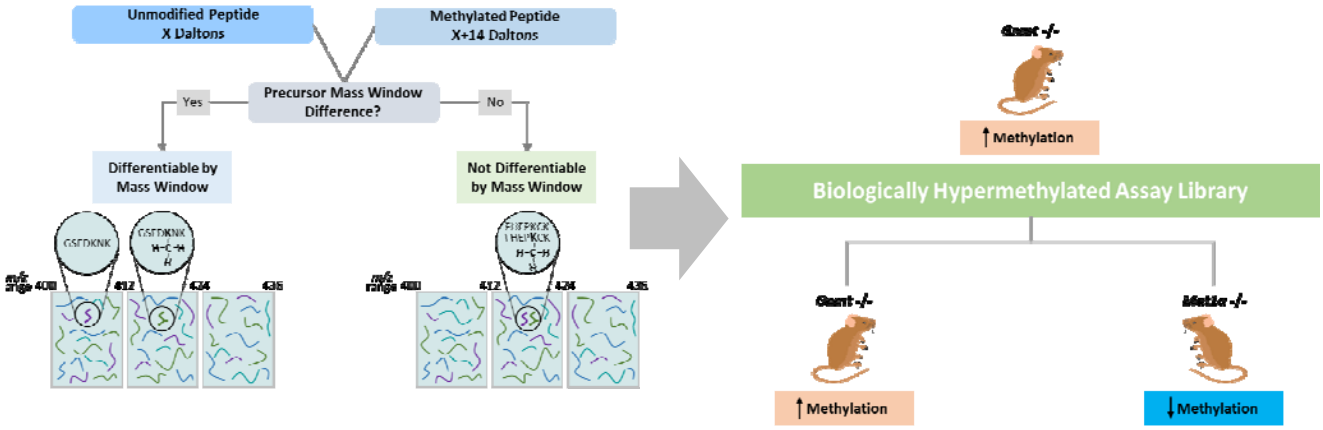

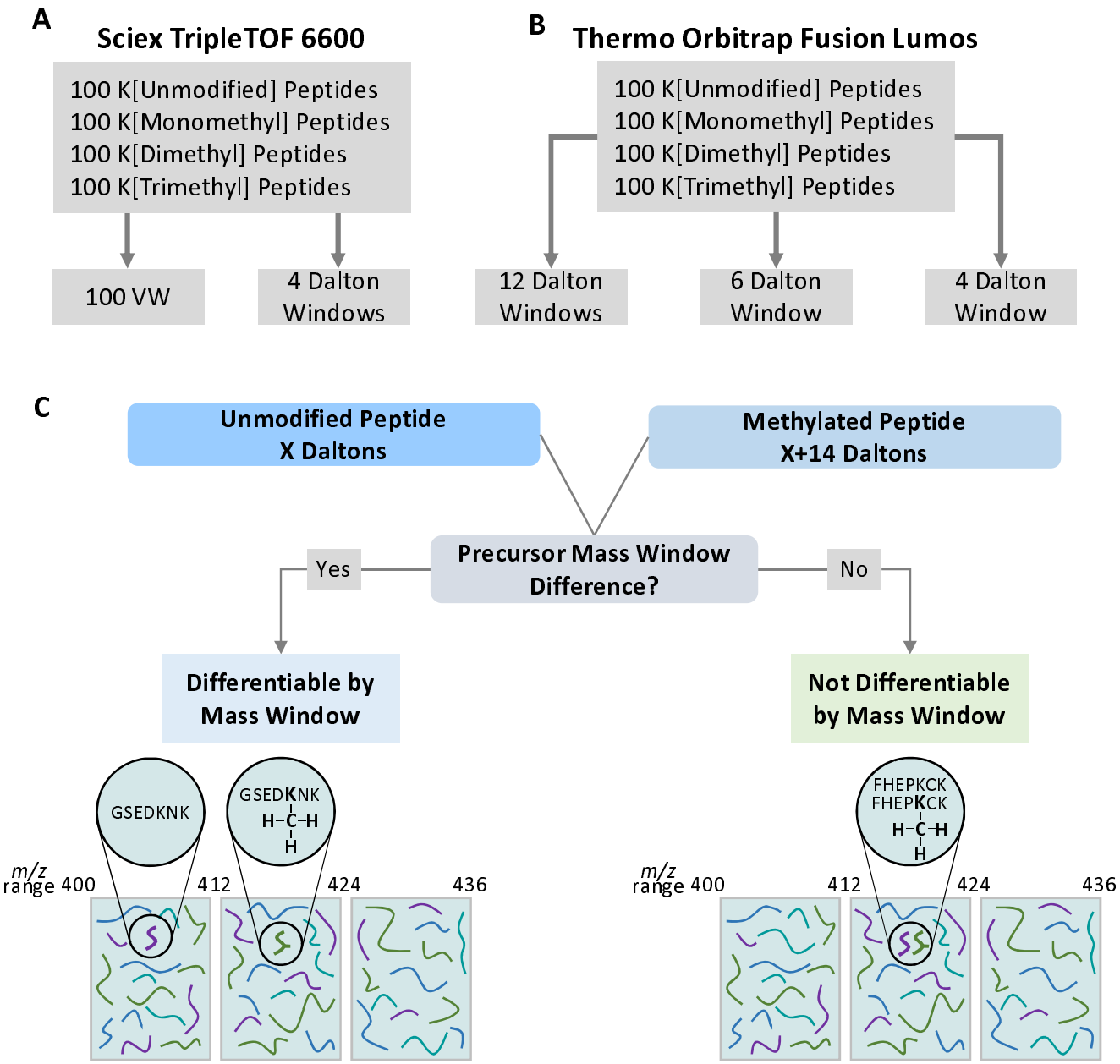

Figure 1. Schematic Overview of Experimental Design:
(A) An equimolar pool of 400 synthesized peptides containing K[Unmodified], K[Monomethyl], K[Dimethyl], and K[Trimethyl] residues were acquired in DIA on the Sciex TripleTOF 6600 with 4 Dalton and 100 Variable Window (VW) precursor mass windows. (B) Same peptide pool was acquired in DIA on the Thermo Orbitrap Fusion Lumos with 4, 6, and 12 Dalton precursor mass windows. (C) Strategy to differentiate an unmodified peptide from it's methylated form based off of precursor mass window difference. An unmodified precursor will be fragmented in a different mass window than its methylated form making it differentiable by precursor mass window.

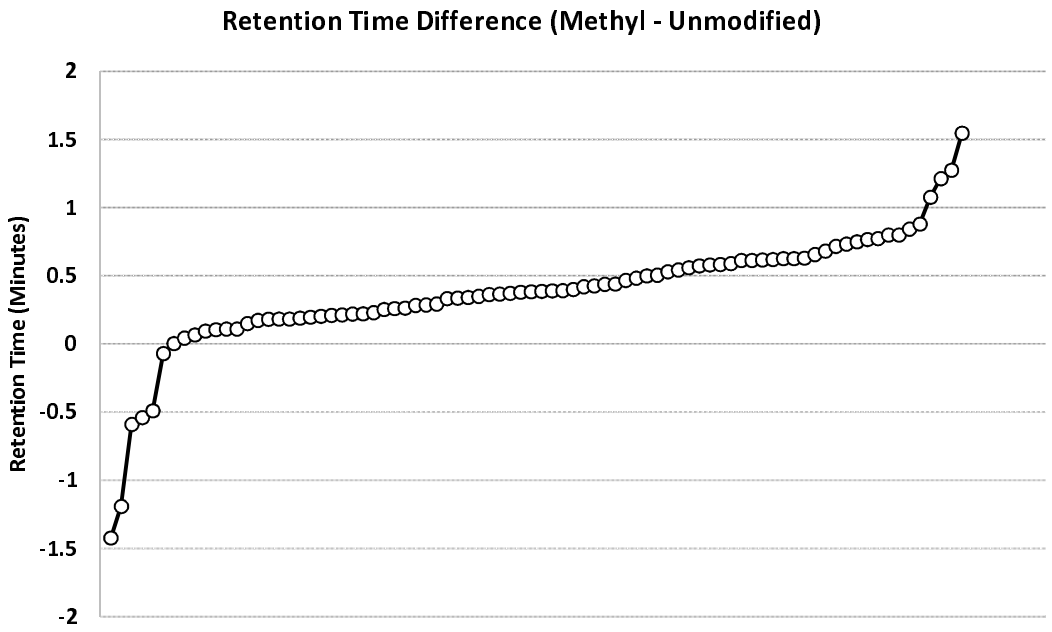

Figure S1. Retention Time Difference Between Methylated and Unmodified Peptide: Difference in retention time of synthesized methylated and unmodified peptides acquired on the Thermo Orbitrap Fusion Lumos in DIA with 4da precursor mass windows with a 60 minute LC gradient Circles represent the retention time of an unmodified peptide subtracted from a methylated peptide

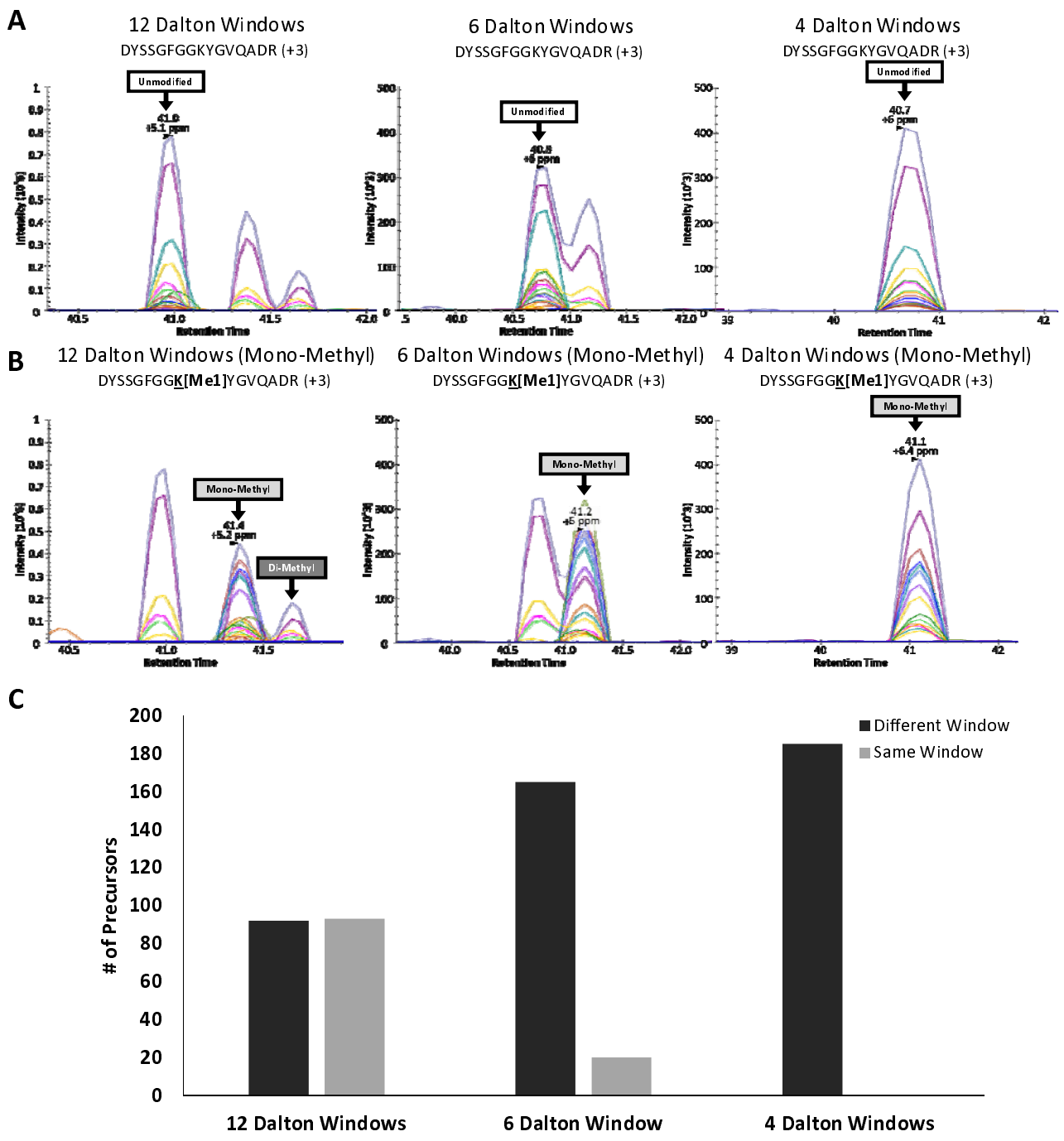

Figure 2. Synthesized Methylated Peptides: Presence of synthesized methylated and unmodified peptides acquired on the Thermo Orbitrap Fusion Lumos with 4, 6, and 12 Dalton precursor mass windows were visualized in Skyline (A) Quantified transitions of DYSSGFGGKYGVQADR (B) Quantified transitions of DYSSGFGG**K[Me1]**YGVQADR (C) Graphical representation of unmodified and monomethyl +2 and +3 precursors which can be differentiated from their unmodified forms using 4, 6, and 12 Dalton precursor mass windows. Black represents peptides eluting in different precursor mass windows while grey represents peptides co-eluting in the same precursor mass window.

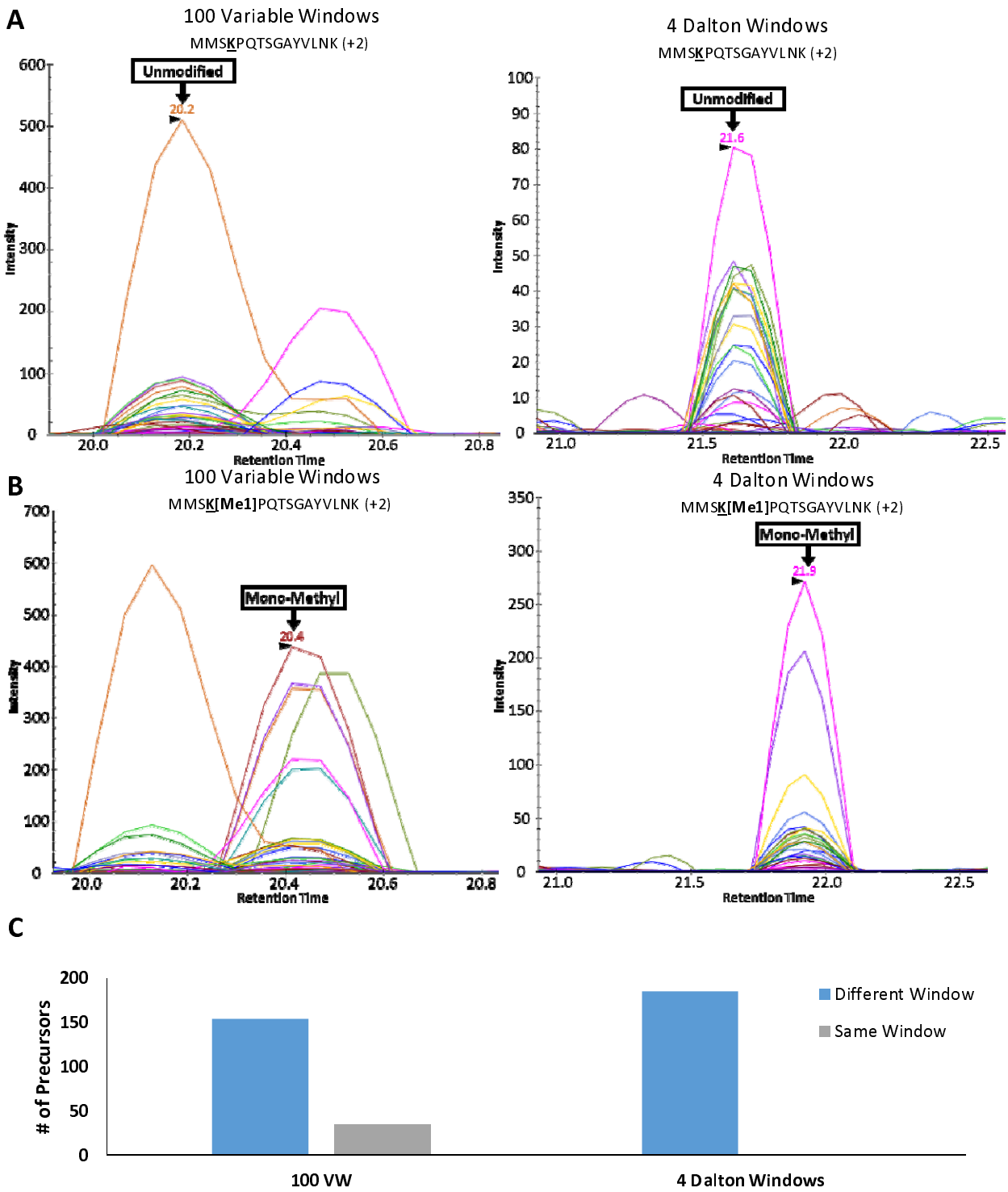

Figure S2. Synthesized Methyl Peptides: Presence of synthesized methylated and unmodified peptides acquired on the Sciex TripleTOF 6600 with 4 Dalton precursor mass windows and 100VW were visualized in Skyline (A) Quantified transitions of MMSKPQTSGAYVLNK. (B) Quantified transitions of MMS**K[Me1]**PQTSGAYVLNK (C) Graphical representation of unmodified and monomethyl +2 and +3 precursors which can be differentiated from their unmodified forms using 4 Dalton and 100VW Precursor Mass Windows. Blue represents peptides eluting in different precursor mass windows while grey represents peptides co-eluting in the same precursor mass window.

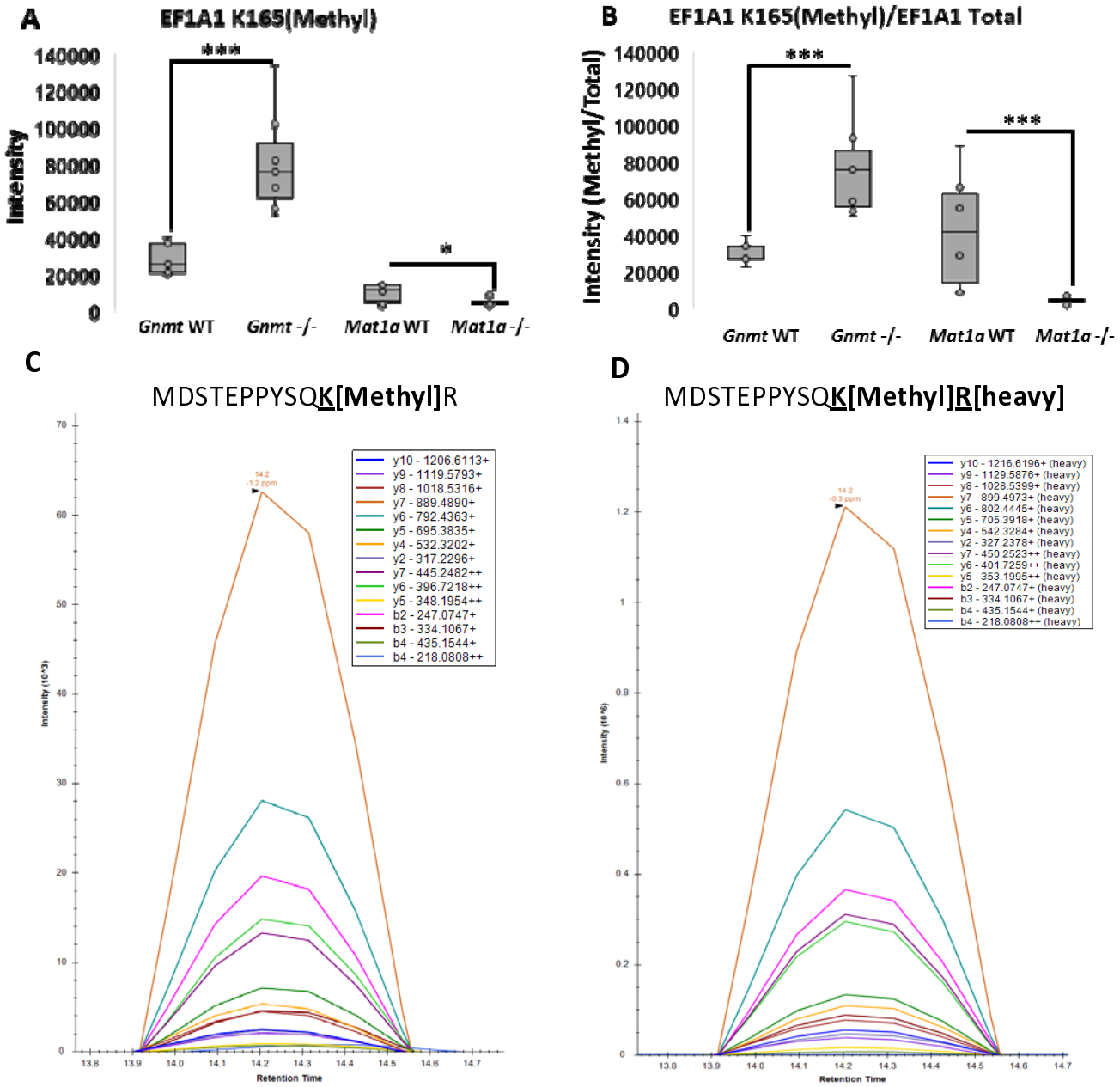

Figure 3. *In-vivo* Methylation: (A) Quantification of the MS2 TIC normalized intensity of peptide containing EF1A1 K[165] Mono-Methyl in *Gnmt* -/- and wild-type littermates and *Mat1a* -/- and wild-type littermates Data are box and whisker plots of six biological replicates. Two-tailed Student's t-test, $^{***}P < 0.005$, $^{*}P < 0.05$ **(**B) Quantification of the intensity of the MS2 TIC normalized peptide containing EF1A1 K[165] Mono-Methyl divided by the intensity of EF1A1 total protein, determined by EF1A1 unmodified peptides using MAPDIA in *Gnmt* -/- and wild-type littermates and *Mat1a* -/- and wild-type littermates Data are box and whisker plots of six biological replicates per condition. Two-tailed Student's t-test, $^{***}P < 0.0005$ (C) Skyline Visualization of the XIC of the peptide MDSTEPPYSQK[Methyl]R which corresponds to EF1A1 K[165] Mono-Methyl in *Gnmt* -/- complex liver lysate (D) Skyline Visualization of the XIC of a stably isotopically labeled peptide MDSTEPPYSQK[Methyl]R[heavy] which corresponds to EF1A1 K[165] Mono-Methyl spiked into *Gnmt* -/- complex liver lysate

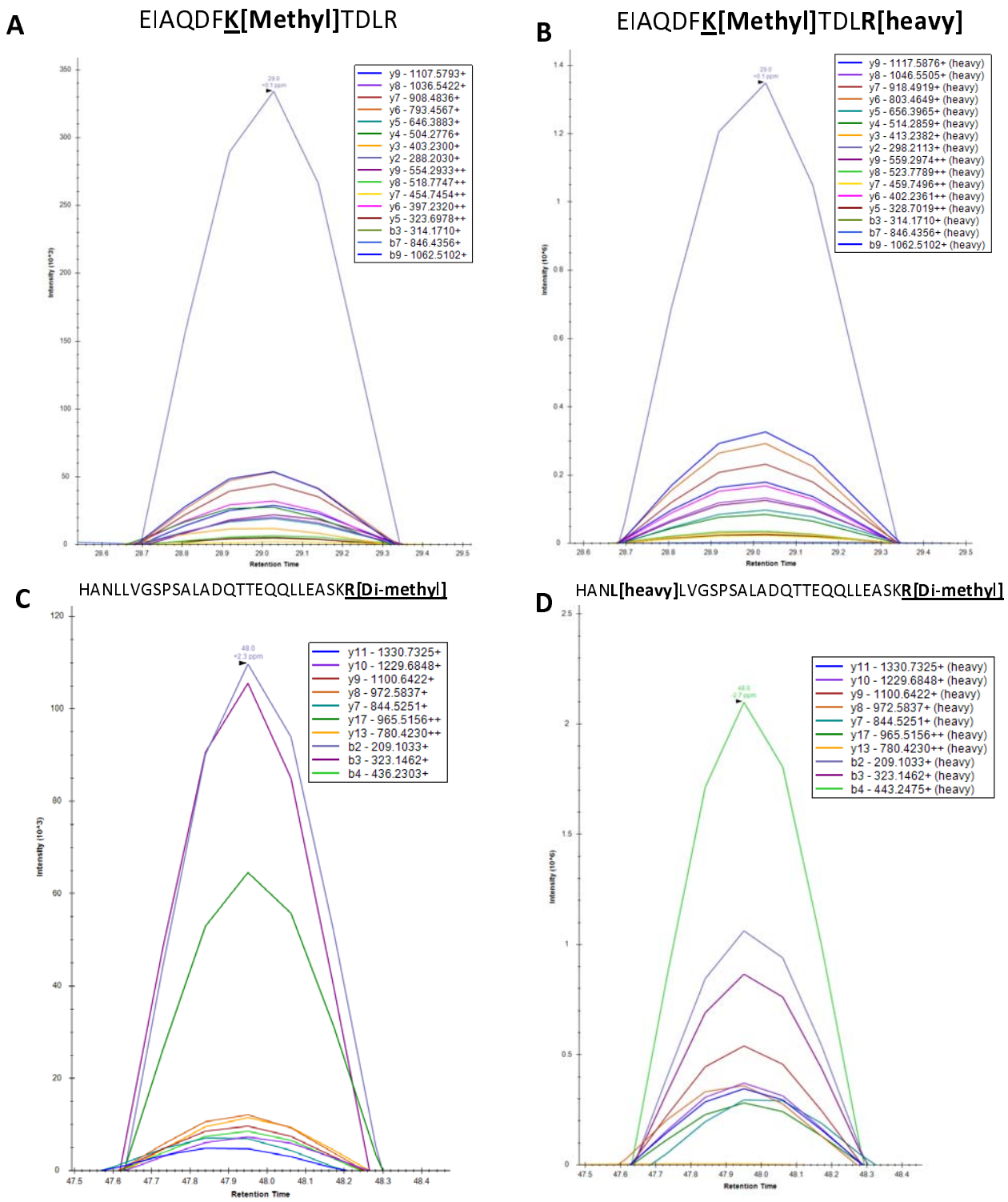

Figure S3. Validation of Methyl Library: Stable Isotopic Labeled methyl-peptides spiked into in *Gnmt* -/- complex liver lysate **(**A) Skyline Visualization of the XIC of EIAQDFK[Methyl]TDLR which corresponds to H3C K[80] Mono-Methyl (D) Skyline Visualization of the XIC of stable isotopically labeled peptide EIAQDFK[Methyl]TDLR[heavy] which corresponds to H3C K[80] Mono-Methyl **(**C) Skyline Visualization of the XIC of HANLLVGSPSALADQTTEQQLLEASKR[Di-methyl] which corresponds to ASPD R[120] Di-Methyl (D) Skyline Visualization of the XIC of stable isotopically labeled peptide EIAQDFK[Methyl]TDLR[heavy] which corresponds to ASPD R[120] Di-Methyl

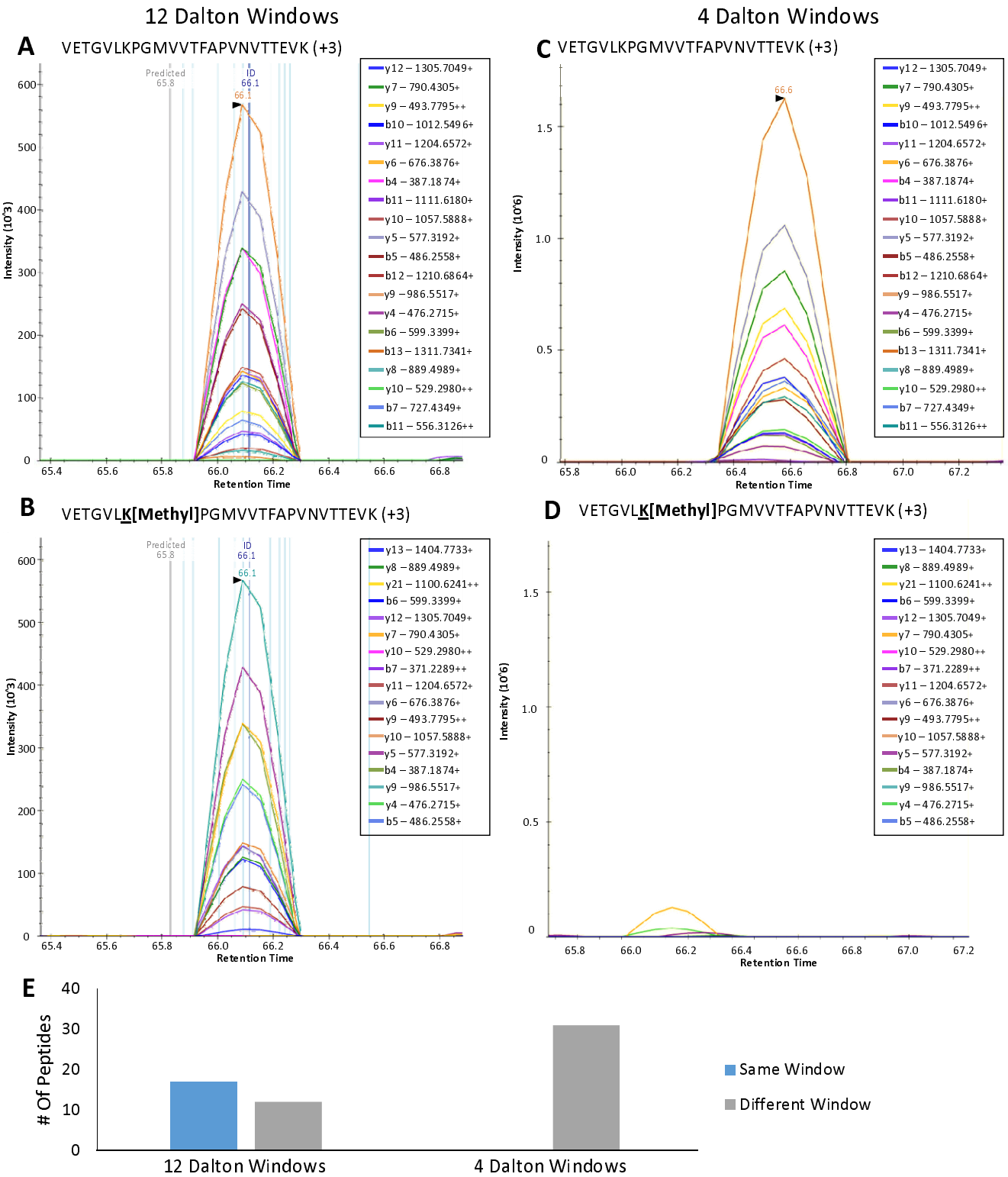

Figure 4. Methylation False Positives: Complex cellular liver lysate from *Mat1a* -/- acquired on the Thermo Orbitrap Fusion Lumos with 4 and 12 Dalton precursor mass windows visualized in Skyline (A) Quantified transitions of VETGVLKPGMVVTFAPVNVTTEVK acquired with 12 Dalton precursor mass window (B) Quantified transitions of VETGVL**K[Methyl]**PGMVVTFAPVNVTTEVK acquired with 12 Dalton precursor

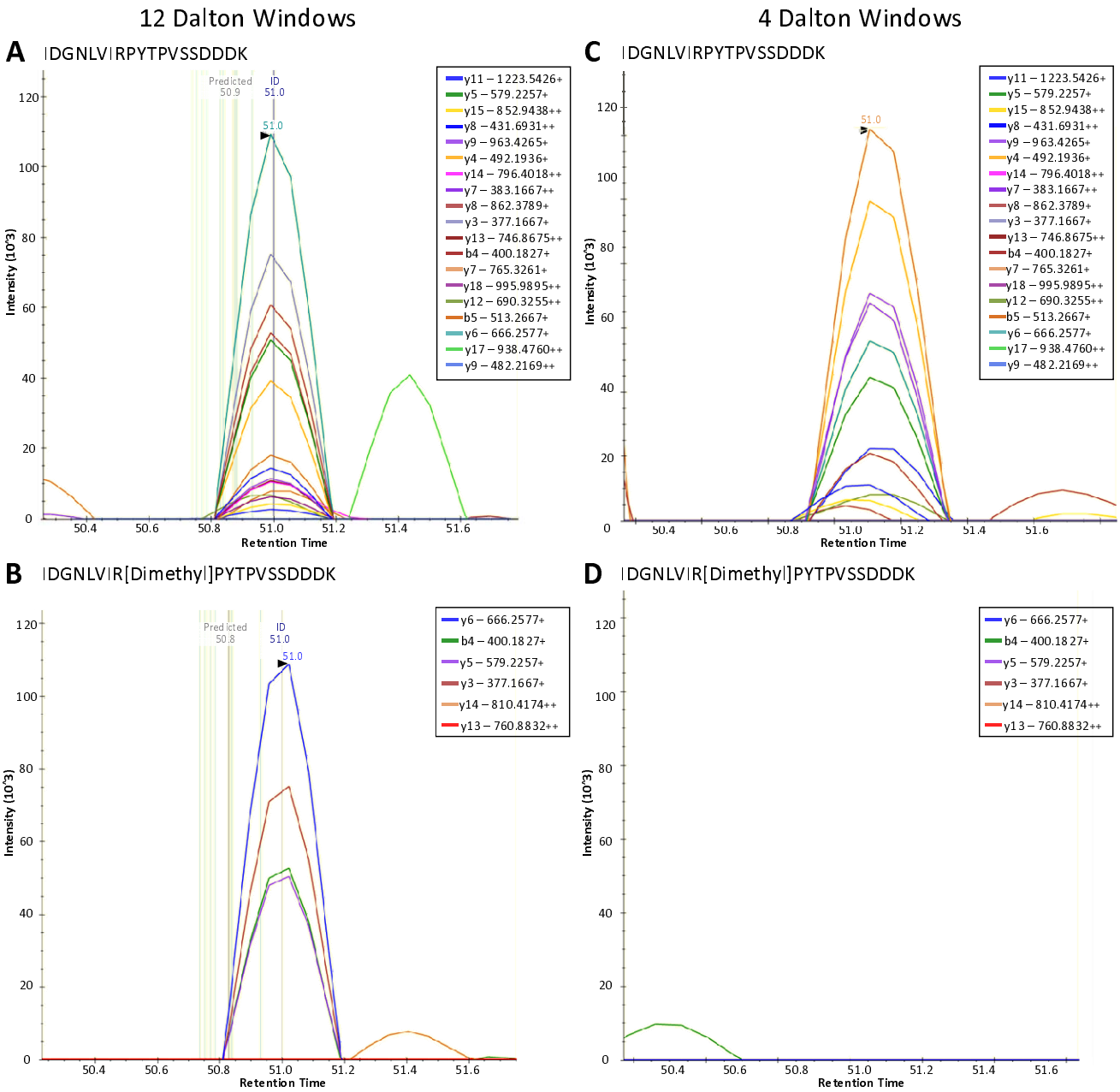

Figure S4. Methylation False Positives: Complex cellular liver lysate from *Mat1a* -/- acquired on the Thermo Orbitrap Fusion Lumos with 4 and 12 Dalton precursor mass windows visualized in Skyline (A) Quantified transitions of IDGNLVIRPYTPVSSDDDK acquired with 12 Dalton precursor mass window (B) Quantified transitions of IDGNLVI**R[Dimethyl2]**PYTPVSSDDDK acquired with 12 Dalton precursor mass windows. This precursor falls in the same mass window as its unmodified form, elutes at the same time, and contains zero site specific transitions, and therefore is a false positive. (C) Quantified transitions of IDGNLVIRPYTPVSSDDDK acquired with 4 Dalton precursor mass window (D) Quantified transitions of IDGNLVI**R[Dimethyl]**PYTPVSSDDDK acquired with 4 Dalton precursor mass windows. There is no discernable peak showing that the methylated peptide found with 12 Dalton precursor mass windows is a false positive This precursor falls in the same mass window as its unmodified form and is a false positive

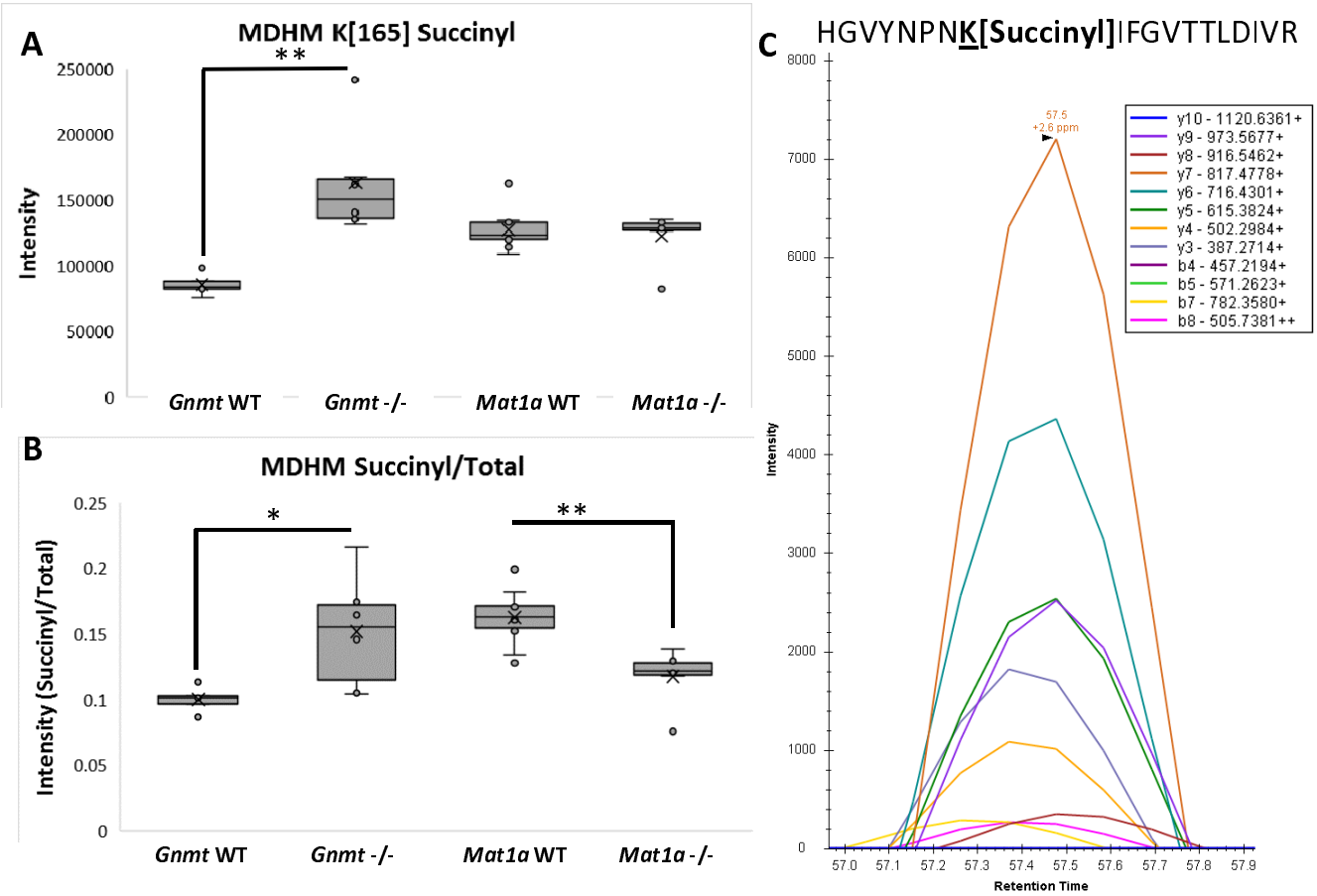

Figure 5. In-vivo Succinylation: (A) Quantification of the MS2 TIC normalized intensity of peptide containing MDHM K[165] Succinyl in *Gnmt* -/- and wild-type littermates and *Mat1a* -/- and wild-type littermates (n=6/condition) Data are box and whisker plots of six biological replicates per condition. Two-tailed Student's t-test, $^{**}P < 0.005$ **(**B) Quantification of the intensity of the MS2 TIC normalized peptide containing MDHM K[165] Succinyl divided by the intensity of MDHM total protein, determined by MDHM unmodified peptides using MAPDIA. Data are box and whisker plots of six biological replicates per condition. Two-tailed Student's t-test, $^{**}P < 0.005$, $^{*}P < 0.05$ (C) Skyline Visualization of the XIC of the peptide containing MDHM K[165] Succinyl

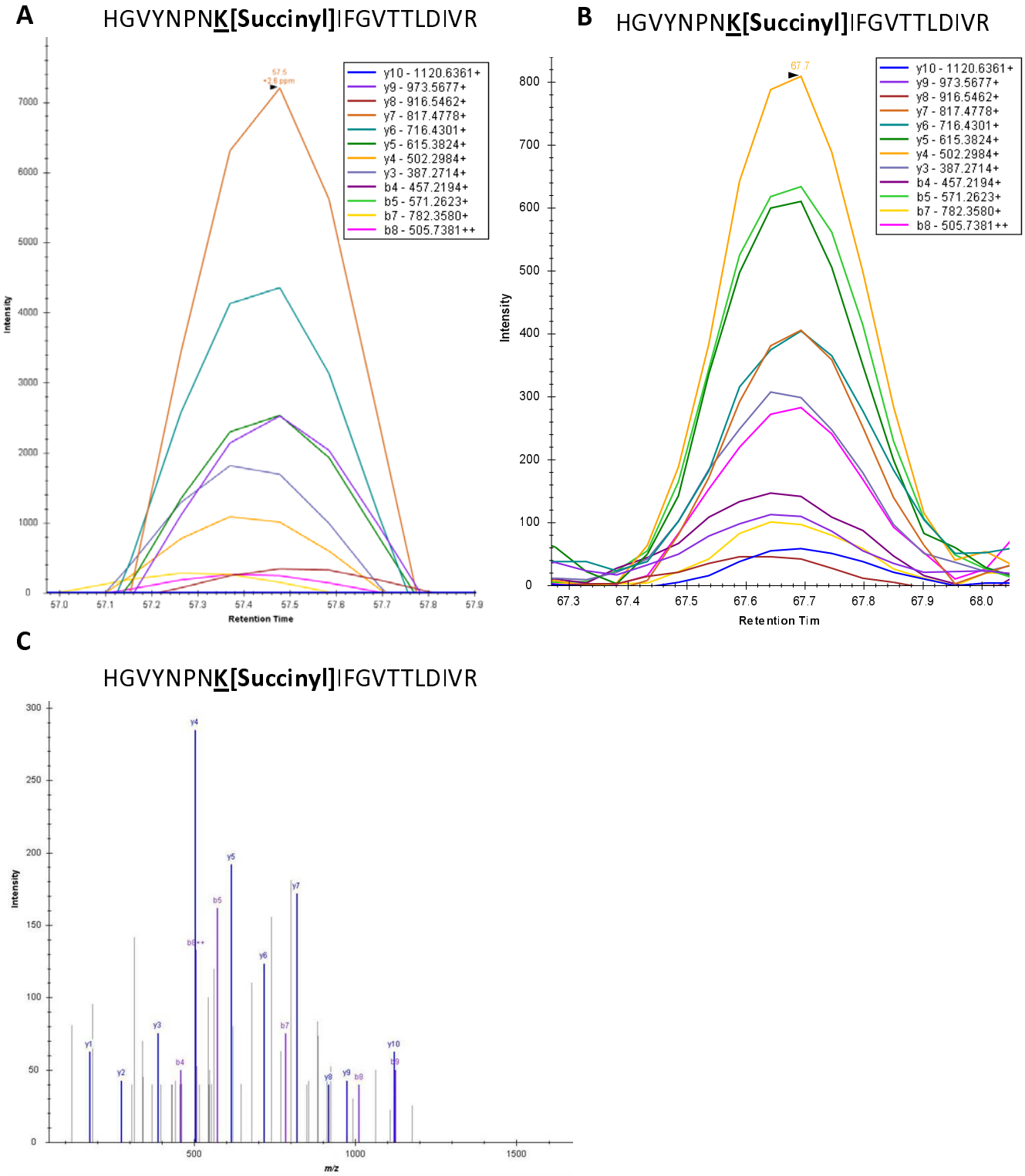

Figure S5. Validation of Succinylation: (A) Skyline Visualization of the XIC of the peptide containing MDHM K[165] Succinyl from *Gnmt* -/- complex liver lysate acquired on an Orbitrap Fusion Lumos **(**B) Skyline Visualization of the XIC of the peptide containing MDHM K[165] Succinyl from a 'one-pot' acetyl-Lys and succinyl-Lys immunoaffinity enrichment from WT mouse liver lysate acquired on a Sciex TripleTOF 6600 (C) Representative spectra of the peptide containing MDHM K[165] acquired on a Sciex TripleTOF 6600

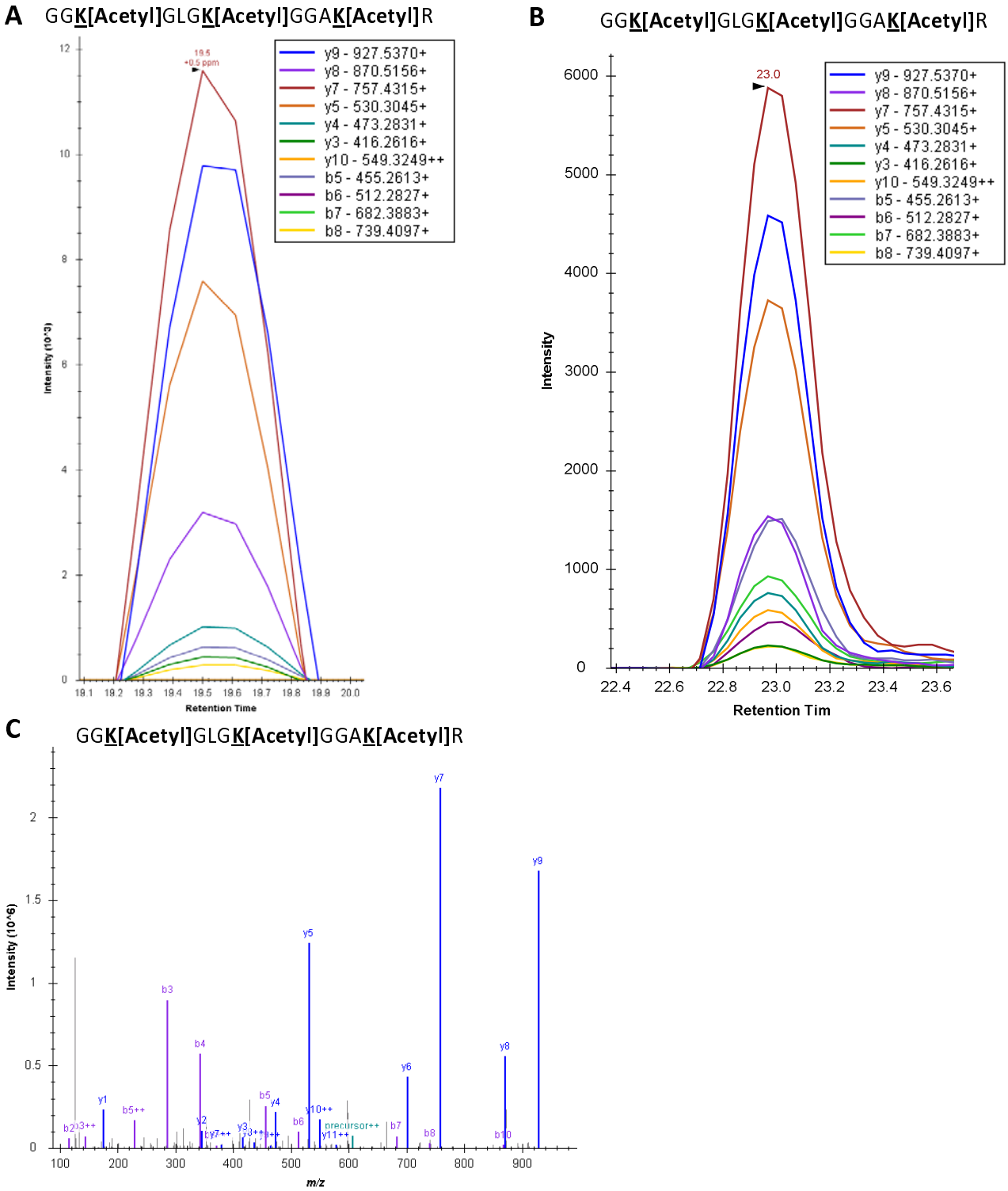

Figure S6. Validation Of Acetylation: (A) Skyline Visualization of the XIC of the peptide containing H4 K[9,13,17] Acetyl in complex lysate from *Gnmt* -/- mouse liver acquired on an Orbitrap Fusion Lumos **(**B) Skyline Visualization of the XIC of the peptide containing H4 K[9,13,17] Acetyl from a 'one-pot' acetyl-Lys and succinyl-Lys immunoaffinity enrichment from WT mouse liver acquired on a Sciex TripleTOF 6600 (C) Representative spectra of the peptide containing H4 K[9,13,17] Acetyl from an acetyl immunoprecipitation acquired on a Sciex TripleTOF 6600

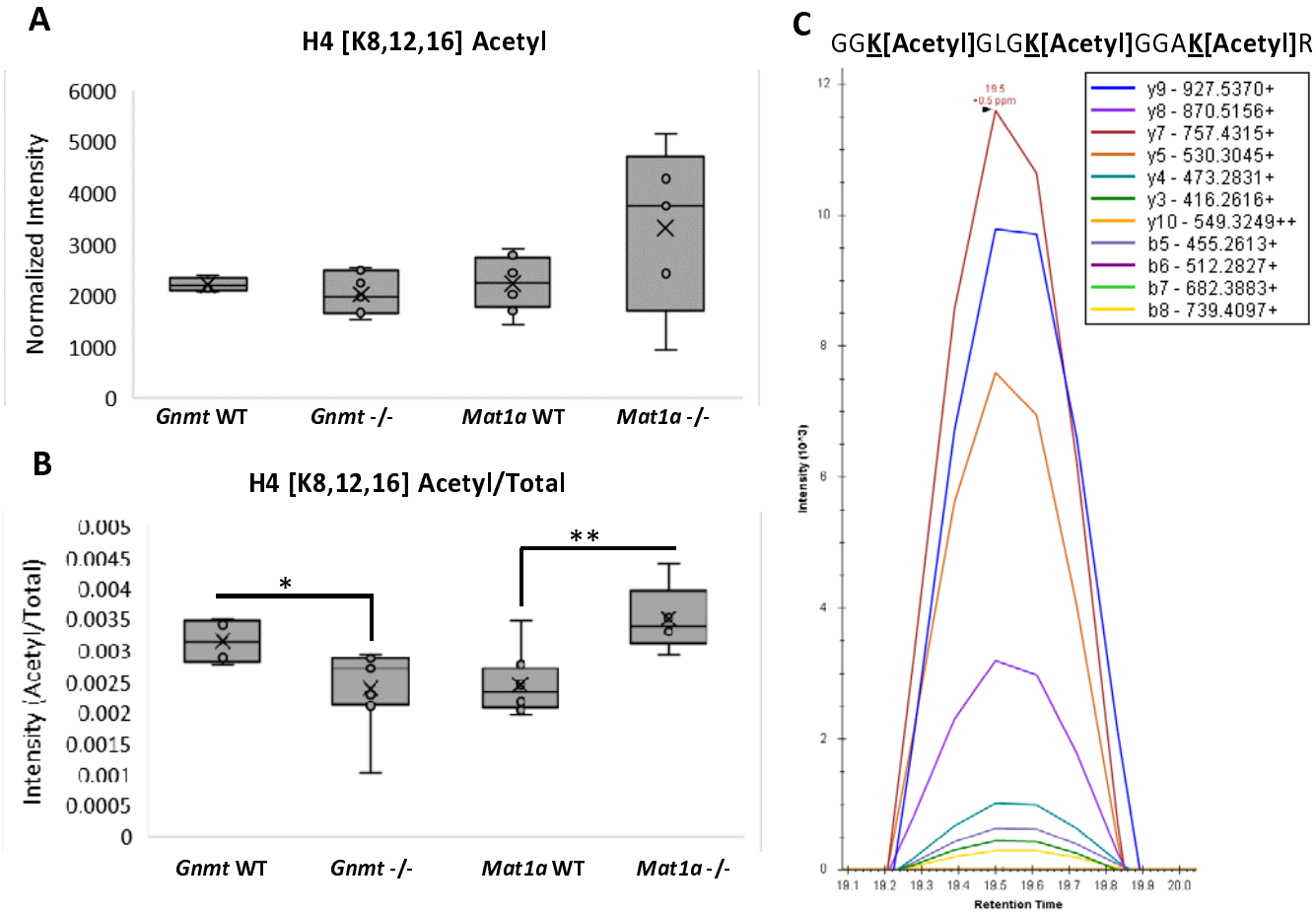

Figure 6. In-vivo Acetylation: (A) Quantification of the MS2 TIC normalized intensity of a proteotypic peptide mapping to H4 K[8,12,16] Acetyl in *Gnmt* -/- and wild-type littermates and *Mat1a* -/- and wild-type littermates. Data are box and whisker plots of six biological replicates per condition. **(**B) Quantification of the intensity of the MS2 TIC normalized peptide containing H4 K[8,12,16] Acetyl divided by the intensity of H4 total protein, determined by H4 unmodified peptides using MAPDIA in *Gnmt* -/- and wild-type littermates and *Mat1a* -/- and wild-type littermates. Data are box and whisker plots of six biological replicates per condition. Two-tailed Student's t-test, $^{**}P < 0.005$, $^{*}P < 0.05$ (C) Skyline Visualization of the XIC of the peptide containing H4 K[8,12,16] Acetyl

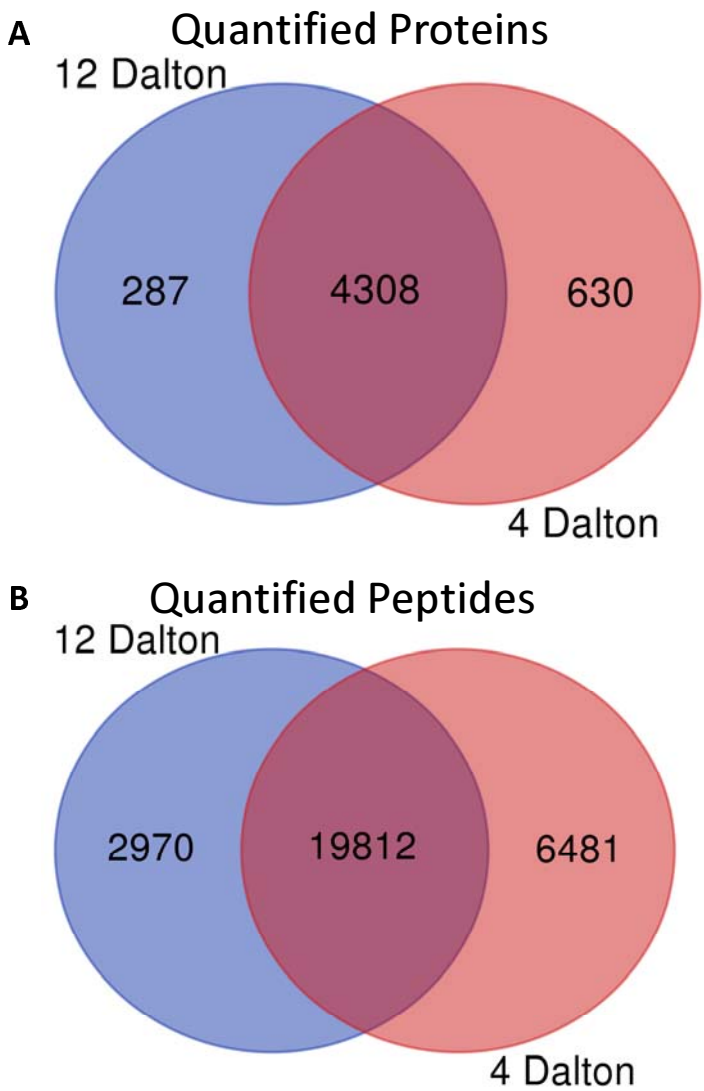

Figure S7. Total Protein Quantitation With 4 and 12 Dalton Precursor Mass Windows: (A) Venn Diagram representing the of overlap between proteins quantified using MAPDIA from the 4 and 12 Dalton Precursor Mass Window DIA acquisitions respectively. Blue represents proteins quantified in 12 Dalton precursor mass window and red represents proteins quantified in 4 Dalton precursor mass windows, (B) Venn Diagram representing the of overlap between peptides quantified using MAPDIA from the 4 and 12 Dalton Precursor Mass Window DIA acquisitions respectively. Blue represents peptides quantified in 12 Dalton precursor mass window and red represents peptides quantified in 4 Dalton precursor mass windows,

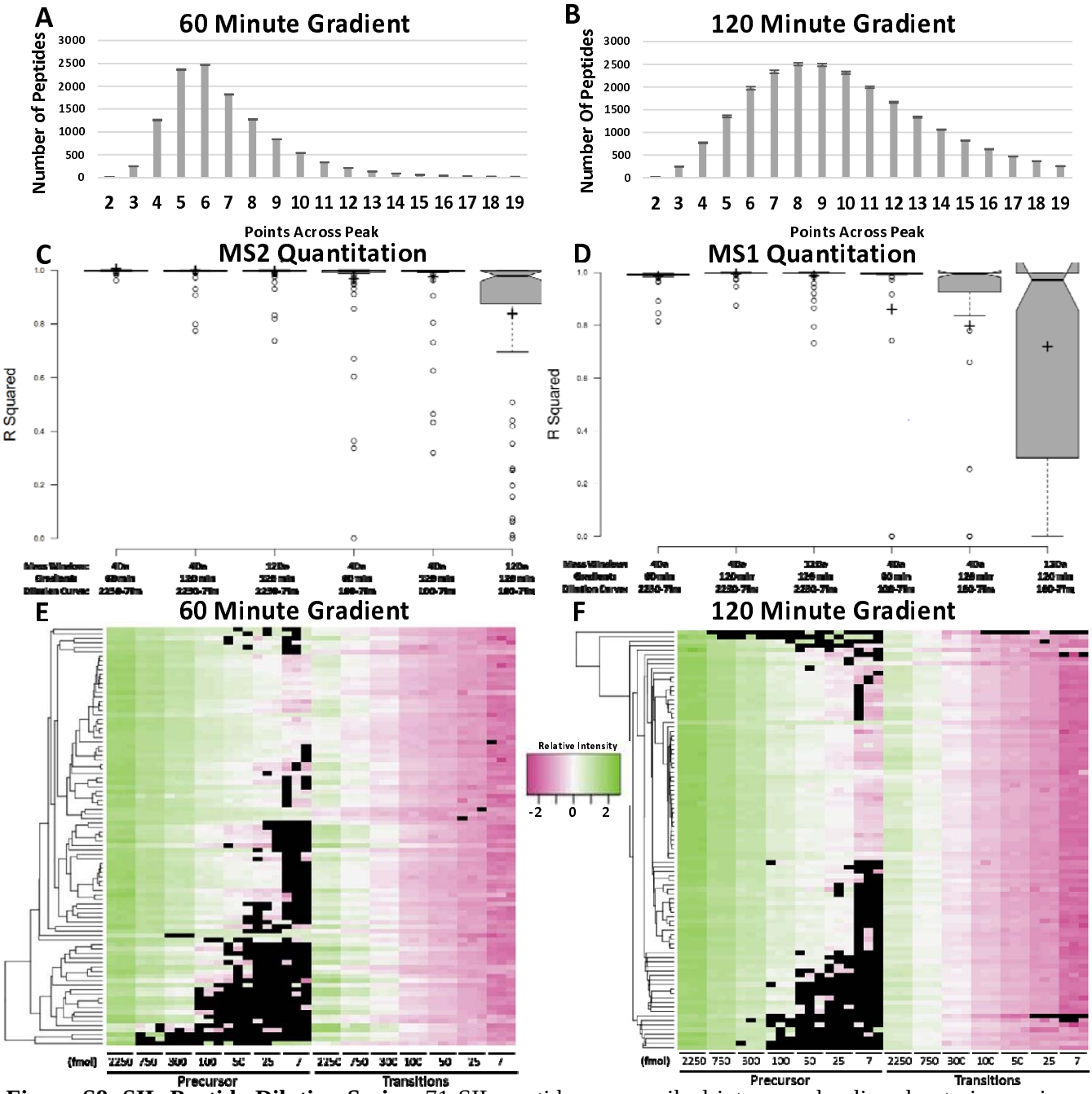

Figure S8. SIL Peptide Dilution Series: 71 SIL peptides were spiked into complex liver lysate in varying concentrations and acquired on the Thermo Orbitrap Fusion Lumos in DIA with 4da precursor mass windows (A) Distribution of points across the chromatographic peak of all endogenous peptides with a 60 minute LC gradient and (B) a 120 minute LC gradient. (C) Box plots showing the accuracy of quantitation using of a dilution series of SIL peptides in complex liver lysate acquired with different DIA acquisition methods and gradients for MS2 quantitation and (D) MS1 quantitation. (E) Heatmap corresponding to intensity of SIL peptides in dilution series with a 60 minute gradient. (F) Heatmap corresponding to intensity of SIL peptides in dilution series with a 120 minute gradient. For A/B: All data are mean ± s.e.m. of three technical replicates. For C/D: For all data, center lines show the medians; box limits indicate the 25th and 75th percentiles as determined by R software; whiskers extend 1.5 times the interquartile range from the 25th and 75th percentiles, outliers are represented by dots; crosses represent sample means. n = 91 SIL precursors. For E/F: Color represents intensity of peptide, black represents missing data. Data is three replicates per concentration of SIL peptides.

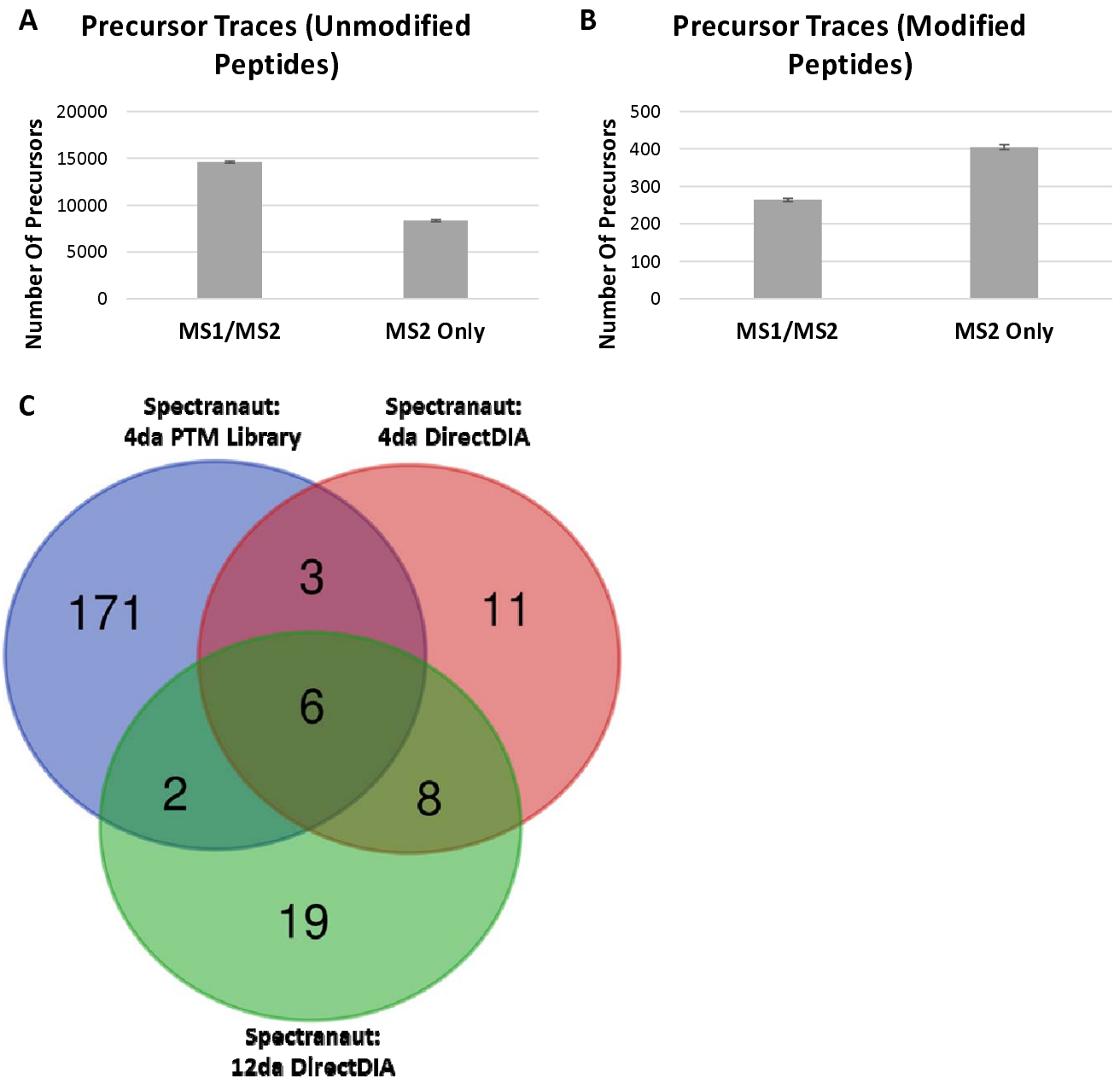

Figure S9. Precursor Traces of Endogenous Peptides: Bar graphs representing peptides identified from complex liver lysate acquired on the Thermo Orbitrap Fusion Lumos in DIA with 4da precursor mass windows with co-eluting precursor trace. (A) Unmodified peptides (B) Modified peptides which contain Mono-, Di-, or Tri-methylated Lys, Acetyl Lys, and Succinyl Lys respectively. All data are mean ± s.e.m. of eight biological replicates. (C) Endogenous modified peptides detected using Spectranaut's software suite which contain Mono-, Di-, or Tri-methylated Lys, Acetyl Lys, and Succinyl Lys respectively. Targeted PTM enriched DIA library based approach was compared to MS1-centric approach (DirectDIA) in both 4 and 12 Dalton precursor mass windows.

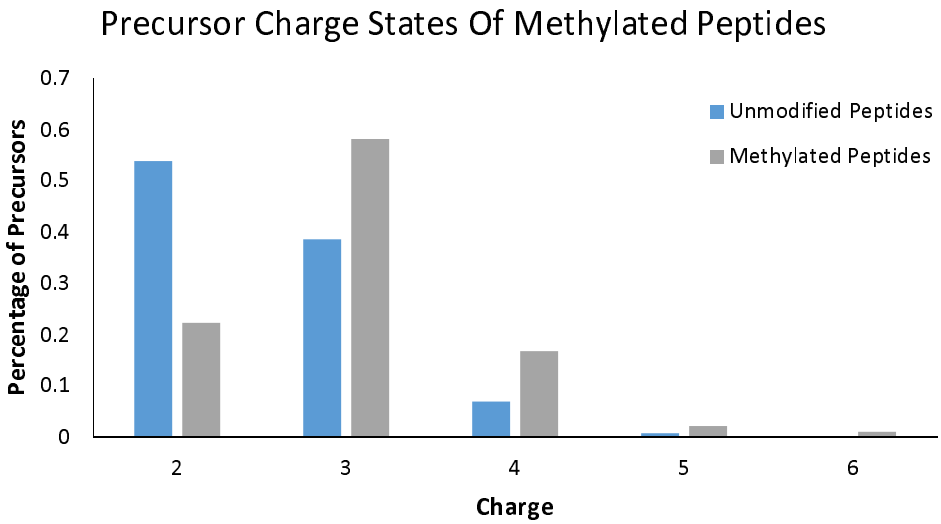

Figure S10. Precursor Charges of Methylated Peptides: Precursor charge states between unmodified and methylated peptides from DDA hyper-methylated peptide assay library. Blue represents unmodified precursors while grey represents methylated precursors.

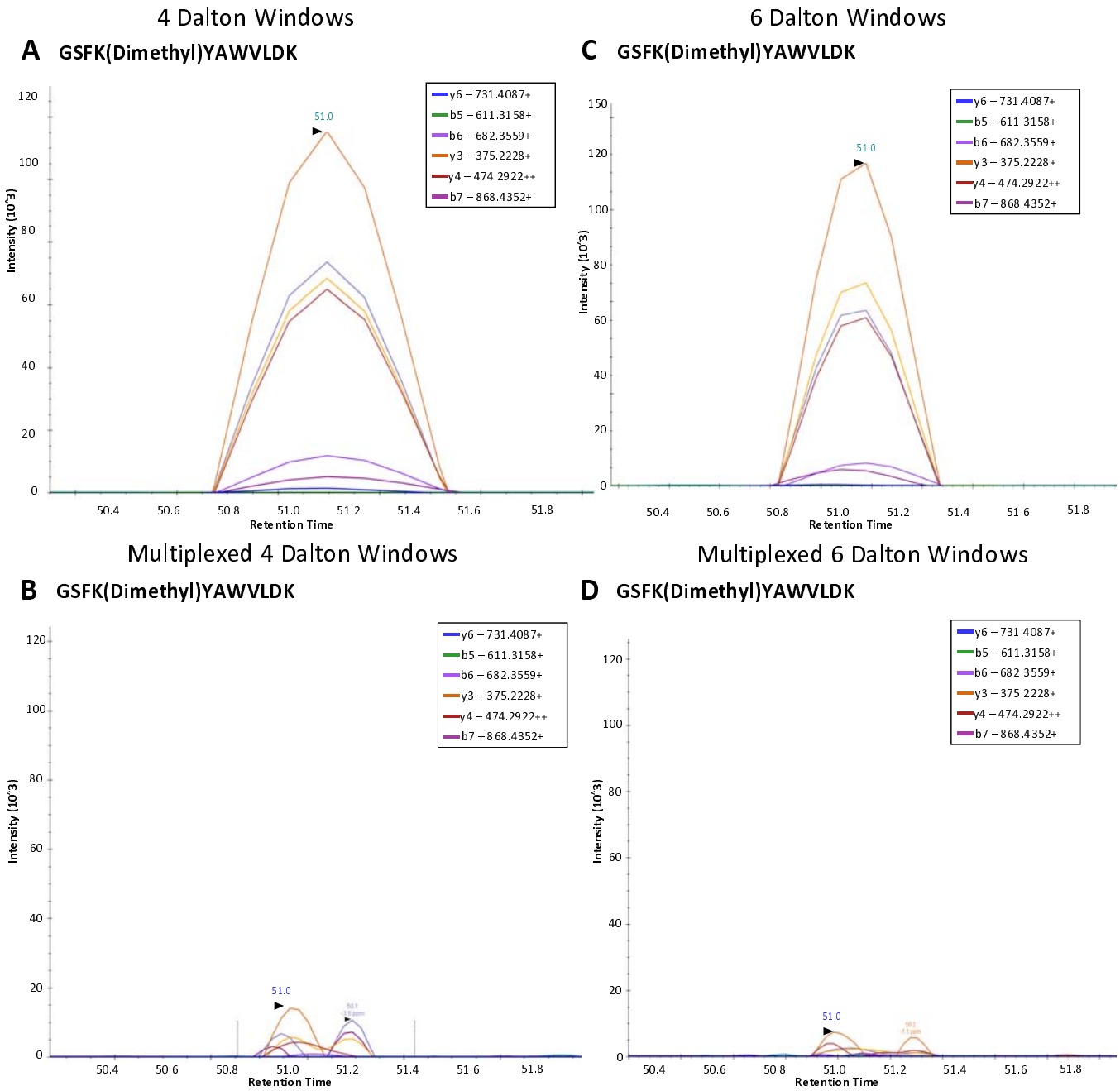

Figure S11. Multiplexed Precursor Mass Windows : Complex cellular liver lysate from *Mat1a* -/- acquired on the Thermo Orbitrap Fusion Lumos with 4 and 6 Dalton precursor mass windows visualized in Skyline (A) Quantified transitions of GSF**K**[Dimethyl]YAWVLDK acquired with 4 Dalton precursor mass window (B) Quantified transitions of GSF**K**[Dimethyl]YAWVLDK acquired with Multiplexed 4 Dalton precursor mass windows. 20 random windows were simultaneously acquired and demultiplexed using Skyline. (C) Quantified transitions of GSF**K**[Dimethyl]YAWVLDK acquired with 6 Dalton precursor mass window (D) Quantified transitions of GSF**K**[Dimethyl]YAWVLDK acquired with multiplexed 6 Dalton precursor mass windows. 20 random windows were simultaneously acquired and demultiplexed using Skyline.

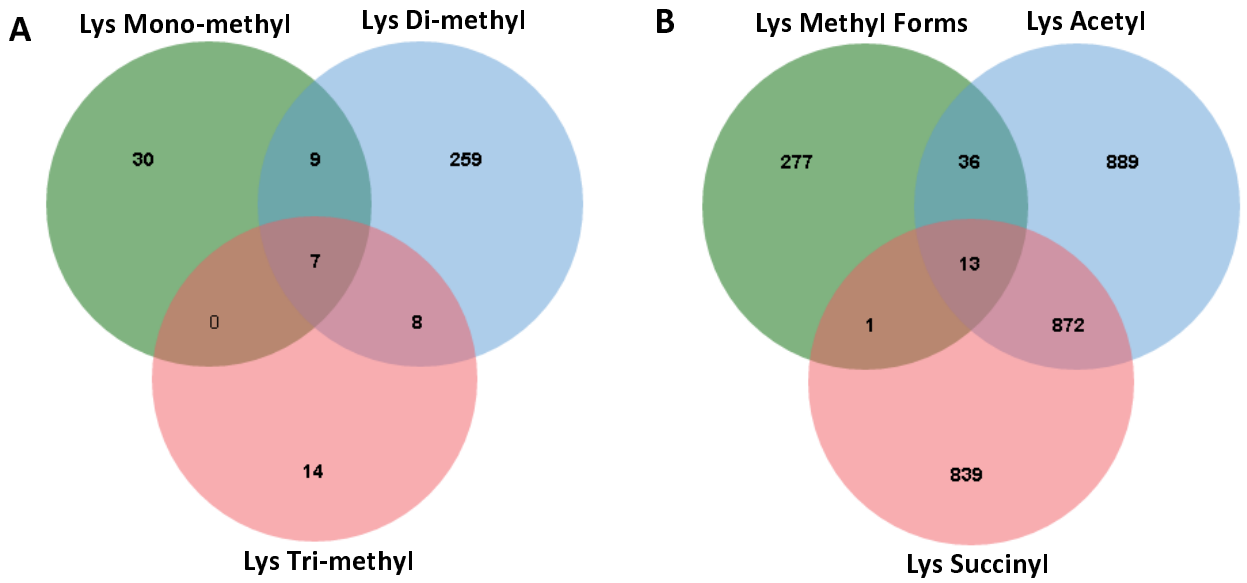

Figure S12. Lysine PTM Crosstalk: Venn Diagrams representing peptides with modified Lys residues. (A) Venn Diagram representing peptides which contain a Mono-, Di-, and Tri-methylated Lys. (B) Venn Diagram representing peptides which contain Mono-, Di-, or Tri-methylated Lys, Acetyl Lys, and Succinyl Lys respectively.